

Simulating low frequency changes in atmospheric CO₂ during the last 740 000 years

P. Köhler and H. Fischer

Alfred Wegener Institute, Helmholtz Center for Polar and Marine Research, P.O. Box 12 01 61, 27515 Bremerhaven, Germany

Received: 15 December 2005 – Published in Clim. Past Discuss.: 14 February 2006

Revised: 3 July 2006 – Accepted: 1 September 2006 – Published: 11 September 2006

Abstract. Atmospheric CO₂ measured in Antarctic ice cores shows a natural variability of 80 to 100 ppmv during the last four glacial cycles and variations of approximately 60 ppmv in the two cycles between 410 and 650 kyr BP. We here use various paleo-climatic records from the EPICA Dome C Antarctic ice core and from oceanic sediment cores covering the last 740 kyr to force the ocean/atmosphere/biosphere box model of the global carbon cycle BICYCLE in a forward mode over this time in order to interpret the natural variability of CO₂. Our approach is based on the previous interpretation of carbon cycle variations during Termination I (Köhler et al., 2005a). In the absence of a process-based sediment module one main simplification of BICYCLE is that carbonate compensation is approximated by the temporally delayed restoration of deep ocean [CO₃²⁻]. Our results match the low frequency changes in CO₂ measured in the Vostok and the EPICA Dome C ice core for the last 650 kyr BP ($r^2 \approx 0.75$). During these transient simulations the carbon cycle reaches never a steady state due to the ongoing variability of the overall carbon budget caused by the time delayed response of the carbonate compensation to other processes. The average contributions of different processes to the rise in CO₂ during Terminations I to V and during earlier terminations are: the rise in Southern Ocean vertical mixing: 36/22 ppmv, the rise in ocean temperature: 26/11 ppmv, iron limitation of the marine biota in the Southern Ocean: 20/14 ppmv, carbonate compensation: 15/7 ppmv, the rise in North Atlantic deep water formation: 13/0 ppmv, the rise in gas exchange due to a decreasing sea ice cover: -8/-7 ppmv, sea level rise: -12/-4 ppmv, and rising terrestrial carbon storage: -13/-6 ppmv. According to our model the smaller interglacial CO₂ values in the pre-Vostok period prior to Termination V are mainly caused by smaller interglacial Southern Ocean SST and an Atlantic THC which stayed before MIS 11 (before 420 kyr BP) in its weaker glacial circulation mode.

Correspondence to: P. Köhler
(pkoeehler@awi-bremerhaven.de)

1 Introduction

Paleo-climatic records derived from ice cores revealed the natural variability in Antarctic temperature (Jouzel et al., 1987), atmospheric dust content (Röthlisberger et al., 2002), and atmospheric CO₂ (Barnola et al., 1987; Fischer et al., 1999; Petit et al., 1999; Monnin et al., 2001; Kawamura et al., 2003; Siegenthaler et al., 2005) over the last glacial cycles. The longest CO₂ record from the Antarctic ice core at Vostok (Petit et al., 1999) went back in time as far as about 410 kyr BP showing a switch of glacial and interglacials in all those parameters approximately every 100 kyr during the last four glacial cycles with CO₂ varying between 180–300 ppmv. New measurements of dust and the isotopic temperature proxy δD of the EPICA Dome C ice core covering the last 740 kyr, however, revealed previous glacial cycles of reduced temperature amplitude (EPICA-community-members, 2004). These new archives offered the possibility to propose atmospheric CO₂ for the pre-Vostok time span as called for in the “EPICA challenge” (Wolff et al., 2004). Here, we contribute to this challenge using BICYCLE, a box model of the isotopic carbon cycle which is based on the interpretation of glacial/interglacial variability of the carbon cycle during Termination I (Köhler et al., 2005a).

The quest of explaining the observed glacial/interglacial variations in atmospheric CO₂ of about 80–100 ppmv (Petit et al., 1999) is challenging the scientific communities for at least two decades (e.g. Archer et al., 2000; Sigman and Boyle, 2000). Processes which need to be included in solving this quest are the transport of organic and dissolved inorganic carbon (DIC) from the surface to the deep ocean via its physical and biological pumps. Large changes in vertical mixing of the water column (Toggweiler, 1999), changes in the strength of the thermohaline circulation (THC) (Knorr and Lohmann, 2003), variations in sea ice cover in high latitudes limiting gas exchange rates (Stephens and Keeling, 2000; Archer et al., 2003) together with well known temperature and salinity variations (Adkins et al., 2002) of the

ocean are processes affecting the carbon cycle via the physical pump. The fertilisation of the marine biological productivity through the aeolian input of iron in areas of high nitrate and low chlorophyll (HNLC) is one theory (Martin, 1990; Ridgwell, 2003b) which would reduce atmospheric CO₂ during glacial times through an enhanced biological export production to the deep ocean. The export of organic carbon itself is closely coupled to the calcium carbonate production of pelagic calcifiers by which CO₂ is released in the surface ocean. Additionally to those processes which distribute DIC, alkalinity and nutrients in the different ocean reservoirs, fluxes of carbon between the terrestrial biosphere and the ocean/atmosphere system (e.g. Joos et al., 2004), riverine input of bicarbonate (Munhoven, 2002), and exchange fluxes of DIC and alkalinity via dissolution and sedimentation of CaCO₃ between ocean and sediments (e.g. Zeebe and Westbroek, 2003) need to be considered to fully understand glacial/interglacial changes in the global carbon cycle.

Previously we put forward a quantitative interpretation of observed changes in atmospheric CO₂ and its carbon isotopes ($\delta^{13}\text{C}$, $\Delta^{14}\text{C}$) using the multi-box model of the global carbon cycle, called BICYCLE, applied to the last glacial termination (Köhler et al., 2005a). That study concluded that the main processes impacting on CO₂ during Termination I were an increase in vertical mixing rates in the Southern Ocean and changes in the DIC and alkalinity inventories through sedimentation and dissolution processes. The time-dependent atmospheric $\delta^{13}\text{C}$ record from the Taylor Dome ice core (Smith et al., 1999) used in that study contains valuable informations, which enabled us to reduce the uncertainties in determining the magnitude and timing of various processes. These results are in that sense robust that the detailed magnitudes of individual processes might vary due to model limitation and data uncertainties, but all their contributions need to be taken into account for explaining the observed variations in the atmospheric carbon records. The novelty of our approach is the simulation in a transient mode. Most other approaches were comparing steady state simulations for different boundary conditions. Assuming that these processes are of general nature, we simulated CO₂ variations with (nearly) the same model over the time period of the last 740 kyr covered by the EPICA Dome C records which represents our contribution to the “EPICA challenge” (Wolff et al., 2005). To this end we forced our model by proxy data from marine and ice core archives. We follow with a sensitivity analysis of the model and discuss its uncertainties.

2 Methods

2.1 The BICYCLE model

The Box model of the Isotopic Carbon cYCLE BICYCLE (Köhler et al., 2005a) was developed and applied for quantitative interpretation of the atmospheric carbon records

(CO₂, $\delta^{13}\text{C}$, $\Delta^{14}\text{C}$) during Termination I (10–20 kyr BP). The model consists of ten oceanic reservoirs in three different depth layers and distinguishes Atlantic, Indo-Pacific and Southern Ocean (Fig. 1). The strength of the preindustrial ocean circulation as seen in Fig. 1 was parameterised with data from WOCE (Ganachaud and Wunsch, 2000). Marine global export production of 10 PgC yr⁻¹ at 100 m water depth (e.g. Gnanadesikan et al., 2002) was prescribed for the preindustrial setting, depending on the preformed macronutrient concentration of PO₄ in the surface waters. In the equatorial regions all macro-nutrients were utilised for the export production, while in the high latitudes the export production flux was restricted to avoid a global export flux of carbon which exceeds the prescribed 10 PgC yr⁻¹. This led to unutilised nutrient concentrations especially in the Southern Ocean, which can be used for increased marine productivity during times of high aeolian iron input into these regions. The global preindustrial export of CaCO₃ was set to 1 PgC (e.g. Jin et al., 2006) with a constant rain ratio of exported organic matter to CaCO₃ of 10:1 throughout all our simulations. The remineralisation of organic matter in the abyss is assumed to follow the denitrification pathway if the deep ocean O₂ concentration drops below 4 $\mu\text{mol kg}^{-1}$, which is in line with the Ocean Carbon-Cycle Model Intercomparison Project (OCMIP) 2 protocol. This implies that during further remineralisation no molecular oxygen is consumed and the model thus avoids unphysical conditions of negative O₂ concentration. During the carbonate compensation (Broecker and Peng, 1987) the response of the sediments to changes in the deep ocean CO₃²⁻ concentration ([CO₃²⁻]) is prescribed with a variable temporal delay (e-folding time τ with τ between 0 and 6 kyr). In doing so we mimic the dissolution or sedimentation of CaCO₃ in the absence of a process-based module of early diagenesis (e.g. Archer et al., 1997, 1998). This leads to net changes in the inventories of DIC and alkalinity and therefore implicitly includes changes in the weathering inputs of bicarbonate through rivers. We are aware of the simplification of this approach, i.e. carbonate compensation in general is a response to balance anomalies in deep ocean [CO₃²⁻] caused by carbon cycle variability of the ocean/atmosphere/biosphere subsystem, the riverine input of alkalinity and its removal by sedimentation. However, while there are evidences for temporal changes in the riverine input rates of bicarbonate (Munhoven, 2002) we are aware of no proxy which can prescribe these changes and have therefore chosen to represent riverine inputs only implicitly in our model. A globally averaged seven-compartment terrestrial biosphere (Köhler and Fischer, 2004) allows photosynthetic production of C₃ and C₄ pathways differing in their isotopic fractionation, and a climate and CO₂-dependent fixation of carbon on land. A more detailed description of the model is found in Köhler et al. (2005a).

It should be noted that carbon dioxide measured in ice cores is in general given as volume mixing ratio in parts per million by volume (ppmv), while carbon cycle models

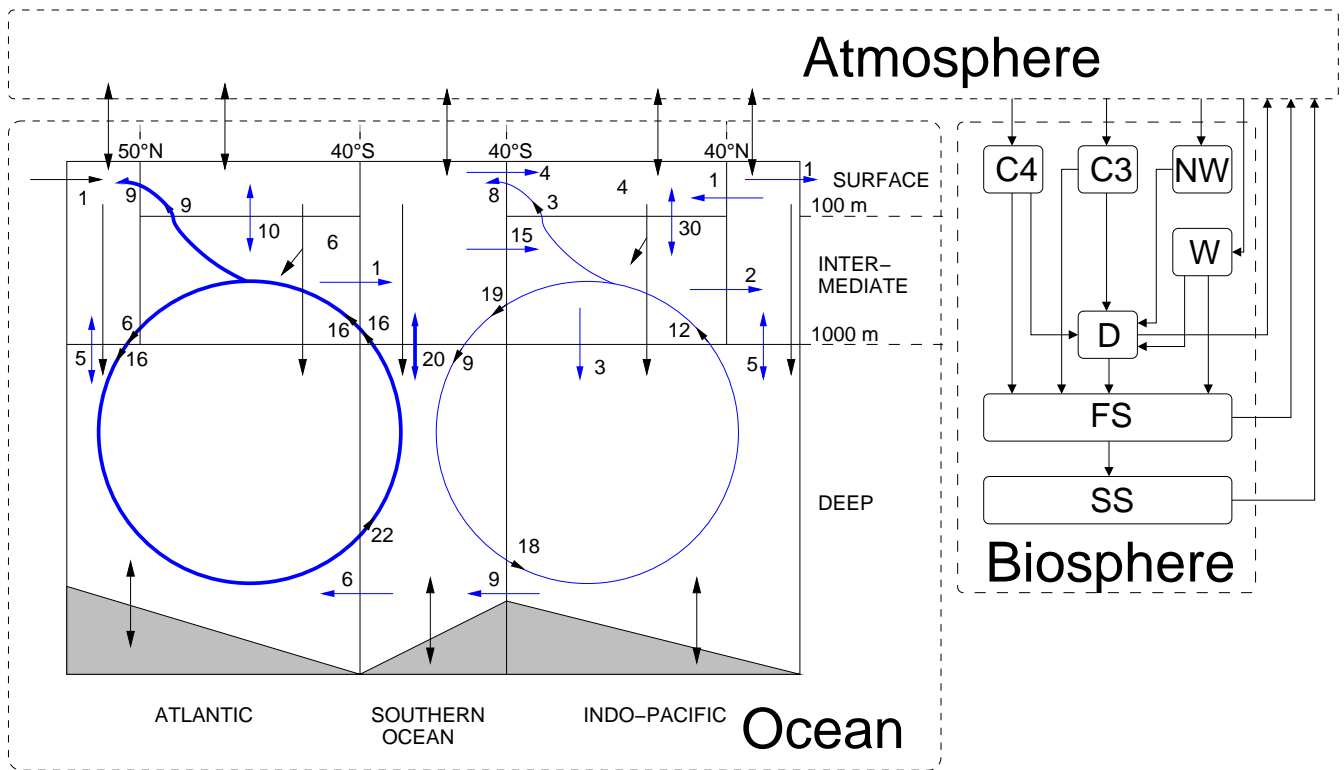


Fig. 1. Geometry of the Box model of the Isotopic Carbon cYCLE (BICYCLE). Carbon fluxes between different reservoirs are shown in black. Biosphere compartments: C4: C₄ ground vegetation; C3: C₃ ground vegetation; NW: non-woody parts of trees; W: woody parts of trees; D: detritus; FS: fast decomposing soil; SS: slow decomposing soil. Ocean: Recent fluxes of ocean circulation (in Sv=10⁶ m³ s⁻¹) are shown in blue based on the World Ocean Circulation Experiment WOCE (Ganachaud and Wunsch, 2000). Bold arrows indicate those fluxes in ocean circulation which are changed over time (NADW formation and subsequent fluxes; Southern Ocean vertical mixing).

calculate the atmospheric partial pressure ($p\text{CO}_2$ in μatm). Only in dry air and at standard pressure, they are identical (Zeebe and Wolf-Gladrow, 2001). For reasons of simplicity we use throughout this article for both carbon dioxide data and simulation results the ice core nomenclature (CO₂ in ppmv) and assume equality between both. This simplification neglects a relatively constant offset between both quantities of a few ppmv.

2.2 Time-dependent forcing of BICYCLE

We forced BICYCLE forward in time using various paleoclimatic records (Fig. 2). The model applied here used the same parameterisation as for its application on Termination I (Köhler et al., 2005a) with some exceptions: (1) We did not consider a complete shut-down of the North Atlantic Deep Water (NADW) formation during Heinrich events. This change is based on productivity results (Sachs and Anderson, 2005) and sea level fluctuations (Siddall et al., 2003) that indicate that Heinrich events during MIS 2 and 3 may have caused different perturbations to the ocean circulation. It is therefore not possible to generalise changes in NADW formation throughout the EPICA Dome C period. Neverthe-

less, we discuss the potential impact of Heinrich events in Sect. 3.3. (2) While we previously prescribed the variability in the depth of the calcite saturation horizon we now assume a time delayed response of the carbonate compensation to changes in the deep ocean [CO₃²⁻]. (3) The aeolian input of iron into the Southern Ocean is now prescribed with an iron flux record published recently (Wolff et al., 2006), and not by the atmospheric dust concentration. The time-dependent forcing used here differs also in some aspects from our initial contribution to the EPICA challenge (Wolff et al., 2005).

Because various records that were used to force our model had a rather coarse resolution we have chosen to smooth all forcing records and all simulation results and concentrate on low frequency changes in the carbon cycle.

The relevant model forcings were used as described in the following:

Ocean temperature: Reconstructed summer SST at ODP980 (McManus et al., 1999; Wright and Flower, 2002) (using modern analogue techniques in the times before 500 kyr (Wright and Flower, 2002)) was used as proxy for SST changes in the North Atlantic (north of 50° N) scaled

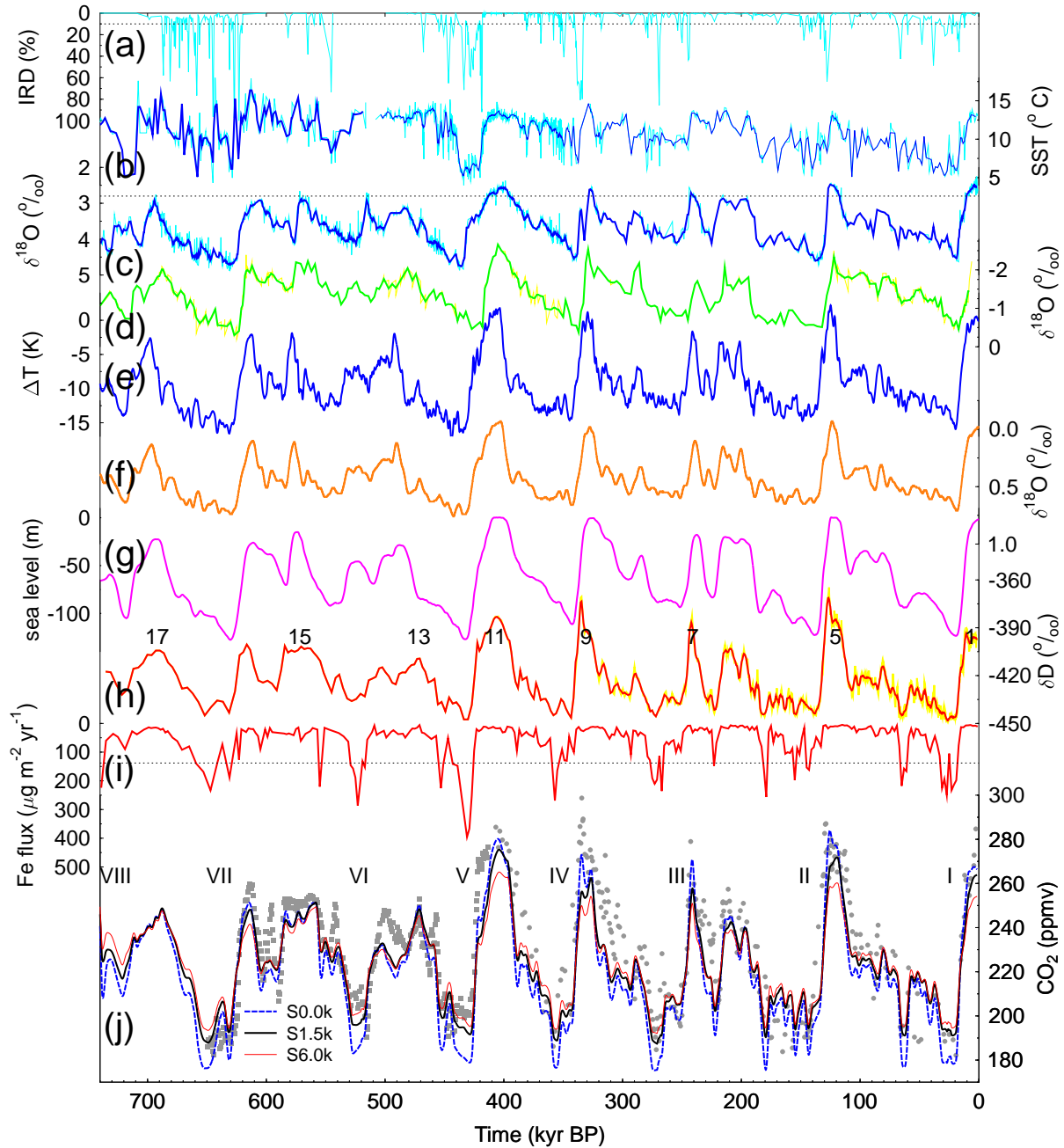


Fig. 2. Paleo-climatic records which were used to force the BICYCLE model (a–i) and measured and simulated CO₂ (j). Ice rafted debris IRD (a), SST reconstructions (b), and benthic $\delta^{18}\text{O}$ in foraminifers (c) from the sediment core drilled at the site ODP980 (55°29' N, 14°42' W) (McManus et al., 1999; Flower et al., 2000; Wright and Flower, 2002). (d): Planktic $\delta^{18}\text{O}$ of ODP677 (1°12' N, 83°44' W) (Shackleton et al., 1990). Reconstructed (e) temperature changes over land in the northern hemisphere (40–80° N), (f) variability in deep ocean $\delta^{18}\text{O}$ caused by deep ocean temperature changes, and (g) sea level changes, (e–g) after Bintanja et al. (2005). Sea level corrected deuterium δD (h) and atmospheric iron fluxes to Antarctica (i) as measured in the EPICA Dome C ice core (EPICA-community-members, 2004; Wolff et al., 2006). (j): Measured CO₂ from Vostok (grey circles) (Petit et al., 1999) plotted on the orbitally tuned age scale (Shackleton, 2000), from EPICA Dome C (grey squares) (Siegenthaler et al., 2005), and simulated CO₂ (lines, 3 kyr running mean) of scenarios with different response time of the carbonate compensation: S0.0K: instantaneous response; S1.5K, S6.0K: response delayed by an e-folding time of 1.5 and 6 kyr, respectively. Data prone to high frequency fluctuations (b, c, d, h) were used as 3 kyr running means. Fe fluxes used as published as 2 kyr averages. Numbers in panel (h) label interglacial MIS, the Latin numbers in panel (j) count the last eight terminations. Horizontal lines (in a, c and i) mark certain thresholds.

to a glacial/interglacial amplitude during Termination I of 4 K (Fig. 2b). SSTs of equatorial surface oceans were estimated from planktic $\delta^{18}\text{O}$ measured in ODP677 in the equatorial Pacific (Shackleton et al., 1990) scaled to a glacial/interglacial amplitude during Termination I of 3.75 K (Visser et al., 2003) (Fig. 2d). Southern Ocean (south of 40° S) SST with a glacial/interglacial amplitude during Termination I of 4 K was estimated from δD of the EPICA Dome C ice core (EPICA-community-members, 2004) (Fig. 2h). The EPICA Dome C δD was corrected for the effect of sea level changes (Jouzel et al., 2003) using a normalised record of sea level change from Bintanja et al. (2005). Deep ocean temperature changes are based on the temperature residual of the benthic $\delta^{18}\text{O}$ (Fig. 2f) calculated by Bintanja et al. (2005) and scaled to a glacial/interglacial amplitude of 3 K (Labeyrie et al., 1987).

Sea ice: Varying sea ice coverage will influence the gas exchange rates between the atmosphere and the surface ocean. We coupled time-dependent changes in the sea ice area in the North Atlantic and the Southern Ocean on the assumed temperature changes in the respective surface ocean boxes. Present day annual mean sea ice area was set to $10 \times 10^{12} \text{ m}^2$ in each hemisphere (Cavaliere et al., 1997). During the LGM the annual average area covered by sea ice increased to $14 \times 10^{12} \text{ m}^2$ in the North and $22 \times 10^{12} \text{ m}^2$ in the South based on various studies (Crosta et al., 1998a,b; Sarnthein et al., 2003; Gersonde et al., 2005). In addition to changing surface box area due to sea level change this results in a relative areal coverage of 50 and 85% in the North Atlantic box and 13 and 30% in the Southern Ocean box during preindustrial times and the LGM, respectively.

Sea level: We used the results of Bintanja et al. (2005) on changes in sea level (Fig. 2g). This modelling study is based on a benthic $\delta^{18}\text{O}$ stack from 57 globally distributed sediment cores covering more than the last 5 million years (Lisiecki and Raymo, 2005). The sea level process combines what is normally called the “salinity effect” (glacial salinity which is about 3% higher than at preindustrial times) with a change in the concentration of DIC, alkalinity, nutrients, and oxygen in the ocean due to variable reservoir sizes. For each change in sea level the geometry (volume, surface area) of the oceanic reservoirs is revised based upon realistic bathymetric profiles calculated from the Scripps Institute of Oceanography data set (<http://dss.ucar.edu/datasets/ds750.1>), which has a resolution of $1^\circ \times 1^\circ$ and 1 m in the vertical direction.

Ocean circulation: There are data- and model-based evidences for a reduced ocean overturning in the Atlantic and the Southern Ocean, while the glacial circulation in large parts of the Pacific Ocean seemed to have been similar to today (Meissner et al., 2003; Hodell et al., 2003; Knorr and Lohmann, 2003; Broecker et al., 2004; McManus

et al., 2004; Watson and Naveira-Garabato, 2006). It was shown (Flower et al., 2000) that the depth gradient in $\delta^{13}\text{C}$ which is an indicator for the strength in NADW formation is highly correlated with benthic $\delta^{18}\text{O}$. To rely on as few different cores as possible and thus to minimise timing uncertainties we therefore used benthic $\delta^{18}\text{O}$ in ODP980 (McManus et al., 1999; Flower et al., 2000) as a proxy for the strength in NADW formation bearing in mind that this might introduce a possible phase shift of the contribution of changes in NADW formation on CO₂ (Fig. 2c). We defined $\delta^{18}\text{O}_{\text{NADW}}=2.8\text{‰}$ as a threshold for changes in the Atlantic thermohaline circulation. The strength of NADW formation of 16 Sv ($1 \text{ Sv}=10^6 \text{ m}^3 \text{ s}^{-1}$) during interglacial periods ($\delta^{18}\text{O}<2.8\text{‰}$) was based on the World Ocean Circulation Experiment WOCE (Ganachaud and Wunsch, 2000), the strength of 10 Sv during glacial times ($\delta^{18}\text{O}\geq 2.8\text{‰}$) on various modelling studies (e.g. Meissner et al., 2003). The net vertical water mass exchange fluxes in the Southern Ocean was coupled linearly to Southern Ocean temperature changes (which is itself prescribed by the EPICA Dome C δD record) with 29 Sv during preindustrial SST and 9 Sv during the LGM. Southern Ocean deep water ventilation would also be reduced due to the glacial reduction of NADW formation by 6 Sv and its subsequent fluxes. Changing ocean circulation fluxes are depicted by bold blue arrows in Fig. 1.

Marine biota: Due to the prescribed export production fluxes in our reference scenario there exist unutilised macro-nutrients in the Southern Ocean surface waters. In these HNLC areas an increased export production in times of high aeolian iron input might occur as described in the iron fertilisation hypothesis (Martin, 1990; Ridgwell, 2003b). Because of the very low snow accumulation rates in EPICA Dome C, the dominant process for aerosol deposition is dry deposition (Legrand, 1987). Therefore, the flux rather than the concentrations of an aerosol species measured in an ice core is expected to be a measure for its changes in the Antarctic and Southern Ocean atmospheric concentration. We therefore used the recently published iron flux measured in the EPICA Dome C ice core (Fig. 2i) (Wolff et al., 2006) as proxy for the aeolian input of iron into the Southern Ocean which might enhance marine biological productivity there if allowed by macro-nutrient availability. The impact of iron input onto the carbon cycle was deduced for Termination I (Köhler et al., 2005a): CO₂ starts to rise at 18 kyr BP, thus all reductions in the iron proxy prior to that point in time do not imply any iron limitation in the Southern Ocean marine biota. The value at 18 kyr BP for the iron proxy is taken as threshold, above which marine export production in the Southern Ocean was not limited by iron. If the iron proxy falls below this threshold it was assumed that iron would be a limiting factor. Thus, the export production exceeding the interglacial global flux of 10 PgC yr^{-1} was then coupled linearly to iron input. Through this threshold approach the variability in the iron proxy during full glacial conditions (no

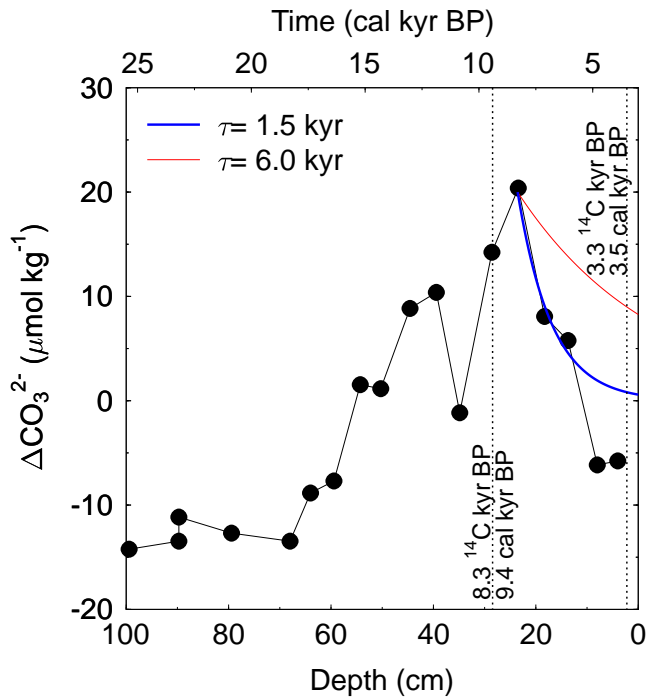


Fig. 3. Reconstructed changes in deep Pacific CO_3^{2-} concentrations after measurements of Marchitto et al. (2005). Vertical lines correspond to age control points to which the time scale was adjusted to. The original radiocarbon ages were transformed into calendar ages using INTCAL04 (Reimer et al., 2004). Relaxation of CO_3^{2-} anomalies based on $N=N_0 \cdot e^{-t/\tau}$ with $\tau=1.5$ or 6.0 kyr.

iron limitation) is negligible and other iron proxies such as dust fluxes or concentrations (EPICA-community-members, 2004) which were used previously lead to similar simulation results.

Terrestrial biosphere: The changing terrestrial carbon storage depends on the internally calculated CO₂ concentration (CO₂ fertilisation) and average global temperature, the latter calculated as 3:1 mixture of northern and southern hemispheric temperature with glacial/interglacial amplitudes of 8 and 4 K, respectively (e.g. Kutzbach et al., 1998). Temperature changes were forced by simulation results from Bintanja et al. (2005) for the North, who calculated the average northern (40–80° N) hemispheric temperature changes as a function of sea level variations and thus northern land ice sheet distribution based on the stacked benthic $\delta^{18}\text{O}$ record of Lisiecki and Raymo (2005) (Fig. 2e), and by EPICA Dome C δD for the South (Fig. 2h). Glacial/interglacial fluctuations in terrestrial carbon is with 400–500 PgC well in the range predicted by various modelling and data based studies (see review in Köhler and Fischer, 2004). Alternative larger glacial/interglacial changes in terrestrial carbon storage are investigated in a sensitivity study.

CaCO₃ chemistry: All changes in the carbon cycle alter $[\text{CO}_3^{2-}]$ in the deep ocean. As a consequence the saturation horizon of CaCO₃ varies, which then induces changes in either the dissolution or sedimentation rates until a new equilibrium is established and the previous deep ocean $[\text{CO}_3^{2-}]$ is obtained again. This process is known as carbonate compensation (Broecker and Peng, 1987). In the absence of a sediment model of early diagenesis, which would cover these processes, we here calculated sediment/deep ocean fluxes of calcium carbonate (changing deep ocean DIC and alkalinity in a ratio of 1:2) by the application of an additional boundary condition. All anomalies in deep ocean $[\text{CO}_3^{2-}]$ from its preindustrial steady state reference values produce CaCO₃ fluxes between sediment and deep ocean to counterbalance these anomalies. This sedimentation/dissolution of calcite reacts not instantaneously to the changes in $[\text{CO}_3^{2-}]$. Their time delayed response to bring $[\text{CO}_3^{2-}]$ back to its initial value can be approximated by an e-folding time τ , which is so far not determined accurately. While modelling studies (Archer et al., 1997, 1998) suggest a τ of approximately 6 kyr, an e-folding time calculated from the paleo reconstruction of deep Pacific variability in $[\text{CO}_3^{2-}]$ (Marchitto et al., 2005) covering the last glacial/interglacial transition is of the order of 1.5 kyr (Fig. 3). We therefore show simulations with different τ : In the scenario S0.0K carbonate compensation responses instantaneously ($\tau=1$ yr), the sedimentary response is significantly delayed in the scenarios S1.5K ($\tau=1.5$ kyr) and S6.0K ($\tau=6.0$ kyr). This approach covers changes in the net fluxes of DIC and alkalinity, and thus implicitly includes riverine inputs of bicarbonate through weathering (Munhoven, 2002), however, there potential temporal variability is not covered here and might be an area for future improvements.

3 Results

In the following the results of simulated atmospheric CO₂ with different response time of the carbonate compensation (scenarios S0.0K, S1.5K, S6.0K) are analysed first (Sect. 3.1), followed by a closer look onto the CaCO₃ chemistry (Sect. 3.2), before we deepen the understanding of our model with a broad sensitivity analysis (Sect. 3.3).

3.1 Simulated low frequency changes in atmospheric CO₂

The simulated atmospheric CO₂ in our three scenarios (Fig. 2j, Fig. 4) shows a similar variability as the CO₂ data sets measured in Vostok and EPICA Dome C ($r^2=0.75-0.76$) (Petit et al., 1999; Siegenthaler et al., 2005). The main difference between the scenarios is a shrinking glacial/interglacial amplitude with growing e-folding time of the sedimentary response. S1.5K and S6.0K show rather similar results for glacial climates, but simulate glacial CO₂

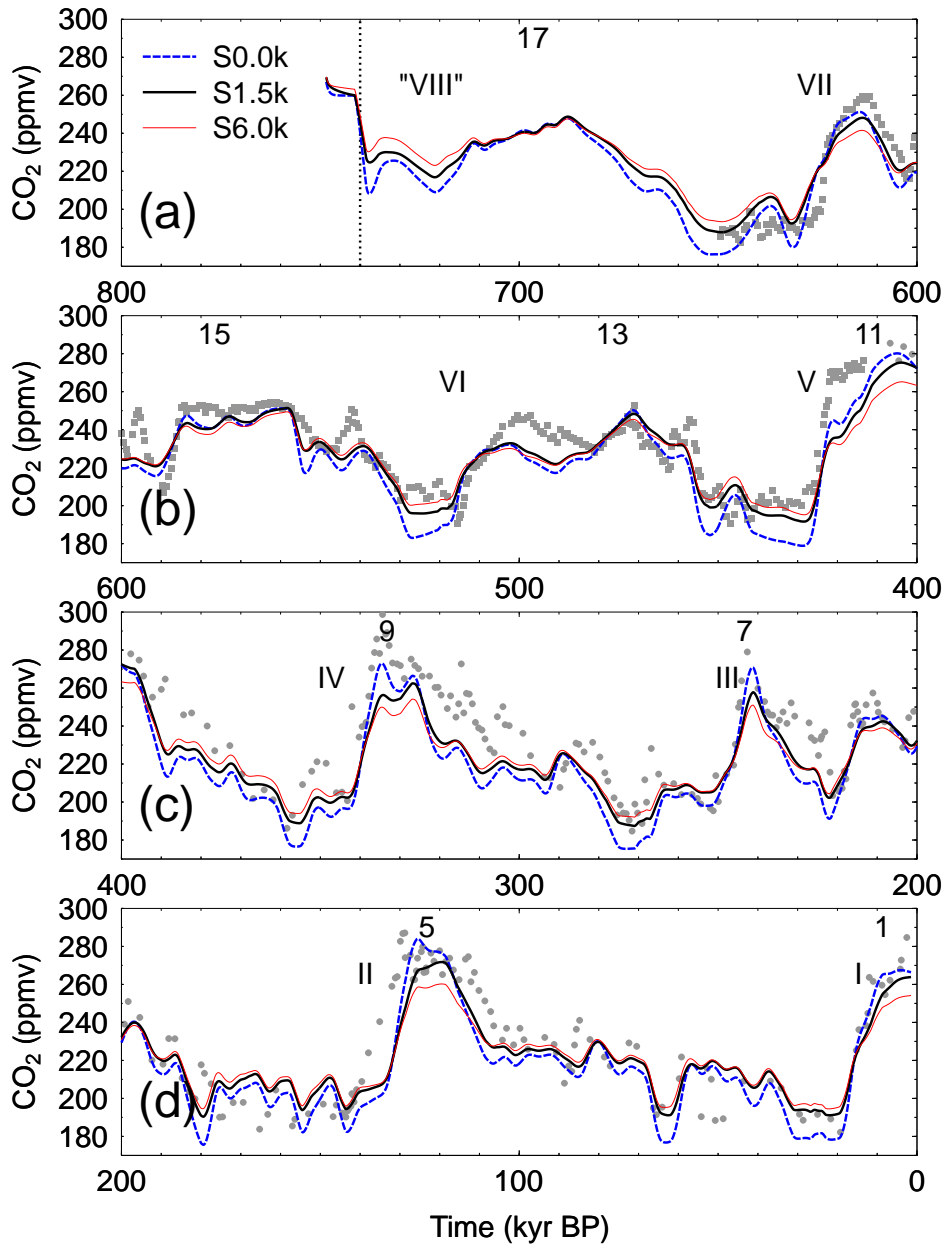


Fig. 4. A detailed view on atmospheric CO₂. (a): 740 to 600 kyr BP. (b): 600 to 400 kyr BP. (c): 400 to 200 kyr BP. (d): 200 to 0 kyr BP. Comparing three different scenarios which differ in the response time of the carbonate compensation: S0.0K: instantaneous response: S1.5K, S6.0K: response delayed by an e-folding time of 1.5 and 6 kyr, respectively. Vostok (grey circles) and EPICA Dome C (grey squares) CO₂ data for comparison. See Fig. 2j for details. Simulations are shown as 3 kyr running mean, dynamics prior to 740 kyr BP (vertical line) are due to model equilibration. MIS of interglacial periods and Terminations (I to VIII) are labelled.

which is up to 15 ppmv higher than during the instantaneous response assumed in S0.0K. During the last five interglacials all three scenarios differ by about 5–10 ppmv with S0.0K simulating the highest, S6.0K the lowest atmospheric CO₂. For reasons of simplicity we concentrate in the following on the scenario with moderate τ (S1.5K) and discuss its results in detail. An in-depth analysis of the causes for the different results of the three scenarios is compiled later-on (Sect. 3.2).

In detail, our model simulates a glacial/interglacial variability in CO₂ as follows (scenario S1.5K): In the Vostok period simulations vary between 190–195 ppmv during glacial maxima and 260–275 ppmv during interglacials in MIS 1, 5, 7, 9, and 11 (Figs. 4c, d). In the pre-Vostok period both the regularity and the amplitude in atmospheric CO₂ as measured in the EPICA Dome C ice core and as simulated with our model differ from those of the Vostok period (Fig. 4a, b).

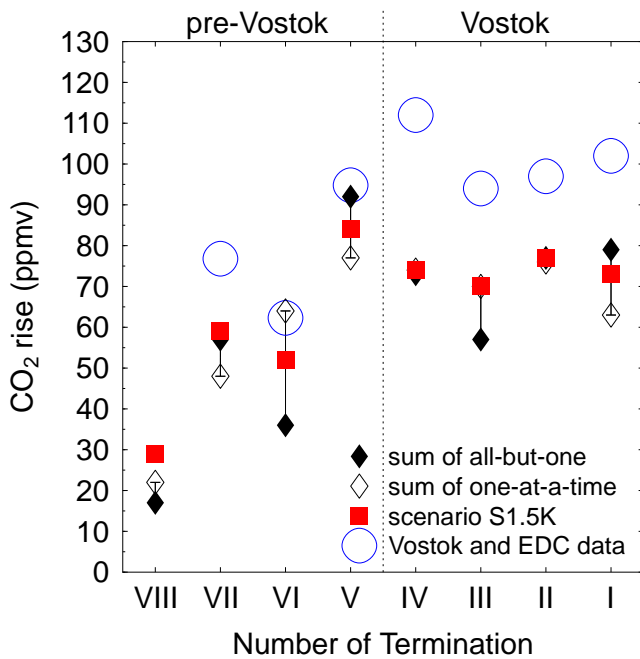


Fig. 5. Estimating the rise in CO₂ between minima and maxima across Terminations I to VIII by various methods. Vostok and EPICA Dome C (EDC) CO₂ data are compared to scenario S1.5K, and to the summation of the two different single process identifications methods used in Fig. 6 (one-process-at-a-time vs. all-but-one-processes).

Peak values during interglacial periods in MIS 13, 15, and 17 reach ~250 ppmv, with 70 to 120 kyr elapsing in-between. Atmospheric CO₂ drops during glacials in MIS 12, 14, and 16 to 190–200 ppmv. The agreement of our simulation results with the measurements in terms of timing is especially good during most terminations (I, III, IV, V, VI), but 10 kyr too late (early) at Termination II (VII). However, it has to be kept in mind, that the uncertainty in the age models of the ice cores are still of the order of thousand years (Vostok CO₂ data are here used on the orbitally tuned age scale of Shackleton, 2000), and the problem of using different paleo records on their individual age scale might introduce cross dating uncertainties into our results. Accordingly significant differences in timing are not surprising.

The glacial/interglacial amplitudes in CO₂ across the last five terminations vary between 70 and 85 ppmv in simulation S1.5K (Fig. 5). This is on average 20–30 ppmv smaller than in the ice core data, with the best and worst agreements for Termination V ($\Delta \approx 10$ ppmv) and IV ($\Delta \approx 40$ ppmv), respectively. The offset between simulations and data is mainly caused by smaller interglacial values in S1.5K. Some peaks in the CO₂ data are represented by single points (e.g. LGM, MIS 7, 9) and might therefore not be representative. Scenario S1.5K simulates the smallest glacial/interglacial rise in CO₂ of 50 ppmv across Termination VI, about two thirds of the

amplitudes simulated across the Terminations I to V; the CO₂ amplitude during Termination VII is of average magnitude (Fig. 5). Termination VIII (CO₂ rise of 30 ppmv in S1.5K, not yet covered by ice core data) has to be taken with caution as EPICA Dome C δD data prior to 740 kyr BP (J. Jouzel et al., unpublished data) reveal that minimum temperatures and thus full glacial conditions in MIS 18 are reached in even older times. The tendency of cooler interglacials as seen in the EPICA Dome C δD data (EPICA-community-members, 2004) is also mirrored by the measured and simulated CO₂ records. The CO₂ concentration in the pre-Vostok period remained longer at relatively high levels, but with smaller CO₂ during interglacials and thus smaller glacial/interglacial amplitudes compared to the Vostok period.

Some major features seen in the CO₂ records, however, are not found in the simulations:

(A) The timing in the simulation of CO₂ reductions during some glaciations is incorrect. This might be caused by an earlier decrease in the Antarctic ice core temperature proxies δD than in the Southern Ocean sea surface temperature (SST). From the deuterium excess record in the ice (Vimeux et al., 2002) it is known that the temperature change in the source regions of the precipitated moisture lags Antarctic temperature during glaciations.

(B) We fail to simulate the CO₂ maxima above 280 ppmv in the last four interglacials (MIS 1, 5, 7, 9). As our model is driven by various paleo-climatic archives plotted on their individual age scales and of low temporal resolution (~1 kyr) especially the simulation of peak values in CO₂ depends on the temporal matching of these driving records. Therefore, our results here have to be understood as an estimate of low frequency fluctuations in CO₂. Furthermore, coral reef growth which increases CO₂ during sea level high stands (Vecsei and Berger, 2004) is not considered so far leaving space for interpretation during interglacial times in which sea level rose above 70 m below present and the main shelves were flooded.

(C) CO₂ rises steep (70 ppmv within 10 kyr) across Termination V into MIS 11 at ~420 kyr BP in the EPICA Dome C data. In the simulation the steep increase is restricted to 45 ppmv followed by a slower rise to full interglacial CO₂. This is partially again mirroring the dynamic of the Antarctic temperature proxy, which shows a slower relative rise than CO₂ during the second half of Termination V (Fig. 2h, j). But this is also caused by the timing of the switch from glacial Atlantic THC to its interglacial strength, a process which is responsible for 15 ppmv of the CO₂ increase (Fig. 6). This latter process depends on the North Atlantic temperature proxy whose relative timing in respect to the paleo-climatic changes recorded in the Antarctic ice cores might be incorrect.

(D) Finally, we do not simulated fast fluctuations in CO₂ as seen in the EPICA Dome C CO₂ record in MIS 15 around 600 kyr BP. At least 20–30 ppmv, about half of the amplitudes seen in the CO₂ record, can be explained, if a more

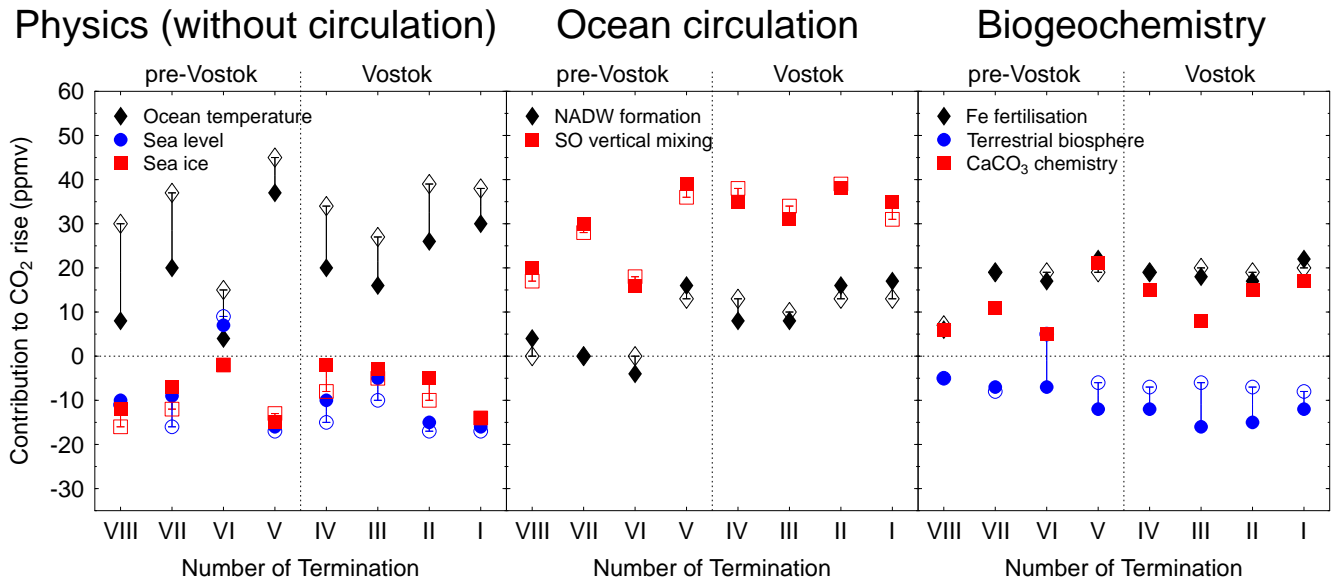


Fig. 6. Impact of different processes on glacial/interglacial changes in CO₂ during the last eight terminations. We estimate single process contributions by either the time-dependent forcing of one process only (open symbols), or by calculating the differences between simulation S1.5K and the simulation which excludes the time-dependent forcing of the process in question (filled symbols). Shown here are the contributions to the CO₂ rise between minima and maxima crossing Terminations I to VIII. Full time-dependent results underlying our analysis here are found in Fig. 7 and Fig. 8. The processes are sub-grouped into physics (excluding ocean circulation), ocean circulation, and biogeochemistry and include changes in ocean temperature, sea level, gas-exchange through sea ice, NADW formation, Southern Ocean vertical mixing, iron (Fe) fertilisation of marine biology in the Southern Ocean, terrestrial biosphere, and DIC and alkalinity fluxes between deep ocean and sediment (CaCO₃ chemistry). Differences between filled and open symbols highlight the high non-linearity of the system. CaCO₃ chemistry (carbonate compensation) is a response process to all other changes in the carbon cycle and cannot be analysed as single effect. The terrestrial carbon storage in the one-at-a-time approach underestimates the effect of CO₂ fertilisation.

accurate and higher resolved record of EPICA Dome C δD (J. Jouzel et al., unpublished data) for the earlier parts of the ice core record is taken to force the model. The uncertainty in the age model in this time period (Brook, 2005) might also be responsible for parts of the offset.

As mentioned by Brook (2005) the EDC2 age model (Schwander et al., 2001) which has been used for all EPICA Dome C records here, might need a revision in the times covering MIS 13 to 15. Our simulations point in the same direction: In general, sea level maxima occur during warm interglacial periods, while sea level minima fall together with minimum temperatures. This is the case for the sea level reconstruction based on benthic $\delta^{18}O$ data (Bintanja et al., 2005) and δD from EPICA Dome C for the last 450 kyr (Fig. 2). During MIS 13 to 15 these two records are out of phase, which is probably caused by chronological uncertainties in the EPICA Dome C records caused by anomalies in ice flow. An updated chronology correcting for these mismatches is currently developed (F. Parrenin et al., unpublished manuscript). The implication of this chronological artefact in the Dome C data sets is, that our reconstruction of CO₂ across Termination VI is biased. For example, the contribution from sea level rise during Termination VI is positive, opposing its signal during all other glacial/interglacial transitions (Fig. 6).

In two sensitivity analyses the importance of individual processes were investigated by (a) forcing only one process at a time (Fig. 7) and (b) excluding one process from time-dependent forcings (Fig. 8). From these analyses we estimate the contributions of individual processes to the rise in CO₂ during the last eight terminations (Fig. 6) keeping in mind the limited validity of the absolute values due to the high non-linearities of the simulated system. In the second approach (simulating all but one processes simultaneously) the process contributions contain also the amplification of the carbonate compensation. Carbonate compensation itself is only a response process to all other changes in the carbon cycle and cannot be analysed in the one-at-a-time approach. Carbon storage on land is a function of atmospheric CO₂ through the CO₂ fertilisation of photosynthesis. The one-at-a-time approach, therefore, depict only changes in the terrestrial carbon pools caused by changes in global temperature, but not by those of the CO₂ concentration. For most processes the two approaches agree within 5 ppmv, only the contribution of the terrestrial carbon pools (12 ppmv) and of the ocean temperature (21 ppmv) have higher uncertainties (Fig. 6).

The contributions (estimated by excluding one process from time-dependent forcings) in decreasing order to the rise in CO₂ are given by Southern Ocean vertical mixing (on average 36 ppmv during Termination I to V and 22 ppmv

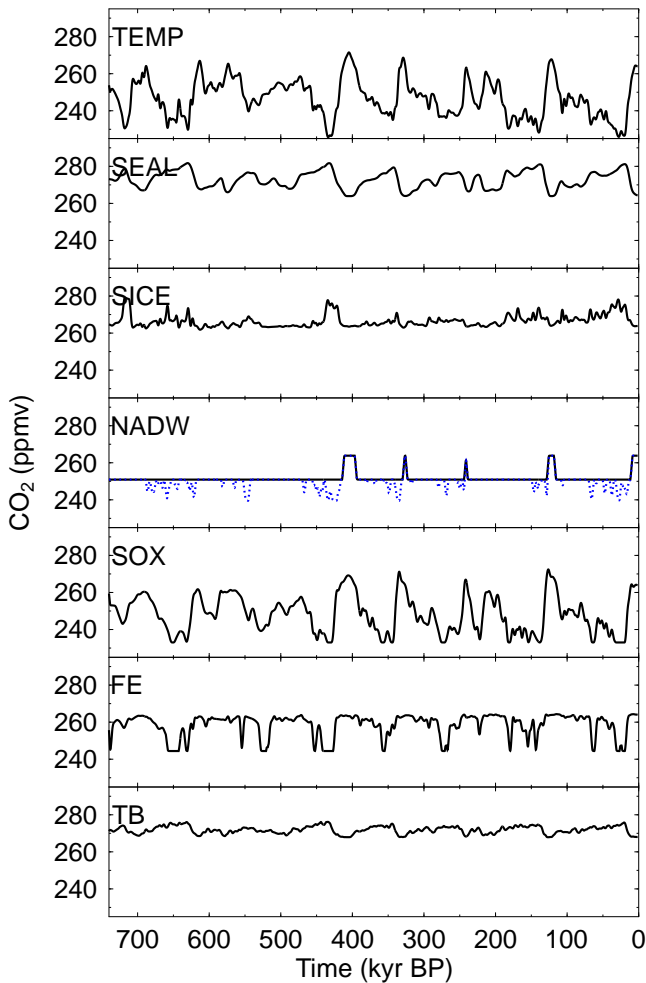


Fig. 7. Analysis of the effect of single processes on atmospheric CO₂. One process at a time was forced externally while all other forcings were held constant at preindustrial level. Considered processes depict changes in ocean temperature (TEMP), sea level (SEAL), sea ice (SICE), NADW formation (NADW), Southern Ocean vertical mixing (SOX), iron fertilisation in Southern Ocean (FE), carbon storage in terrestrial biosphere (TB). Additionally, a scenario with variable NADW formation including its shut-down during Heinrich events is shown (dashed in sub-figure NADW). In TB the effect of CO₂ fertilisation is underestimated due to only small variability in CO₂. Carbonate compensation is a response process to all other changes in the carbon cycle and cannot be analysed as single effect. All simulation results are shown as 3 kyr running mean.

earlier (36/22 ppmv)), ocean temperature (26/11 ppmv), iron fertilisation in the Southern Ocean (20/14 ppmv), the carbonate compensation (15/7 ppmv), and NADW formation (13/0 ppmv). Changes in gas exchange caused by sea ice cover (−8/−7 ppmv), sea level (−12/−4 ppmv), and terrestrial carbon storage (−13/−6 ppmv) were processes enlarging the observed CO₂ rise by up to 33 ppmv during terminations. While most processes are reduced in their magnitude

prior to Termination V, the absolute contribution of iron fertilisation changes only slightly. Thus, the relative importance of biogeochemical processes is enhanced from ~30% (Termination I–V) to ~40% during earlier terminations. Ocean circulation contributes about 60% during all terminations to the CO₂ rise while the contributions of other physical processes (SST, sea level, sea ice) is less than 10% during Terminations I–V and on average neutral earlier (Fig. 6). According to our model the smaller interglacial CO₂ values in the pre-Vostok period prior to Termination V are mainly caused by smaller interglacial Southern Ocean SST and an Atlantic THC which stayed before MIS 11 in its weaker glacial circulation mode.

3.2 A closer look onto the CaCO₃ chemistry

A deeper understanding of the differences in the three scenarios with variable e-folding time of the sedimentary response is obtained by a closer look onto the simulated [CO₃^{2−}] in the deep Pacific Ocean and the total carbon content of the simulated system (Fig. 9). We additionally compare these results with the scenario without carbonate compensation (S–CA) and expected changes in [CO₃^{2−}] during the past 150 kyr based on the conceptual understanding of the carbonate compensation (Marchitto et al., 2005). For the latter case details and timing have to be taken with caution.

The instantaneous responding sediments (S0.0K) preserve a constant [CO₃^{2−}] of 63 μmol kg^{−1} (Fig. 9a). This constancy is paid for by large fluctuations in the total carbon content (Fig. 9b). Total C is up to 1000 PgC larger during glacial periods, which is about 2/3 of the amount of dissolvable CaCO₃ for modern times (1600 PgC) (Archer, 1996). In the other extreme case of no CaCO₃ chemistry (S–CA) total C is preserved, but the [CO₃^{2−}] of the deep Pacific ocean drops during full glacial conditions by almost 25 mmol kg. Both scenarios with reasonable e-folding time of the carbonate compensation lead to variability in total C and deep Pacific [CO₃^{2−}] somewhere between those of the extreme cases: [CO₃^{2−}] varies up to 10 and 14 μmol kg^{−1} around the preindustrial value in S1.5K and S6.0K, respectively. The variability in total C is restricted to 700 PgC (S1.5K) and less than 350 PgC (S6.0K), which is about 2/3 and 1/3 of the variability during instantaneous response. The total C at *t*=0 kyr BP is still 50, 100, and 400 PgC higher in S0.0K, S1.5K and S6.0K, respectively, than during steady state for preindustrial conditions. In other words, in the transient simulations which include the carbonate compensation the carbon content at preindustrial times differs from observational-based estimates by up to 1%. At the end of the glacial or interglacial periods the simulated system in S1.5K and S6.0K is yet not in equilibrium due to the delayed sedimentary response.

Based on a conceptual understanding of the CaCO₃ compensation mechanism the variability in deep ocean [CO₃^{2−}] should start during large changes in the carbon cycle (e.g. during terminations) with a sharp change (rise during

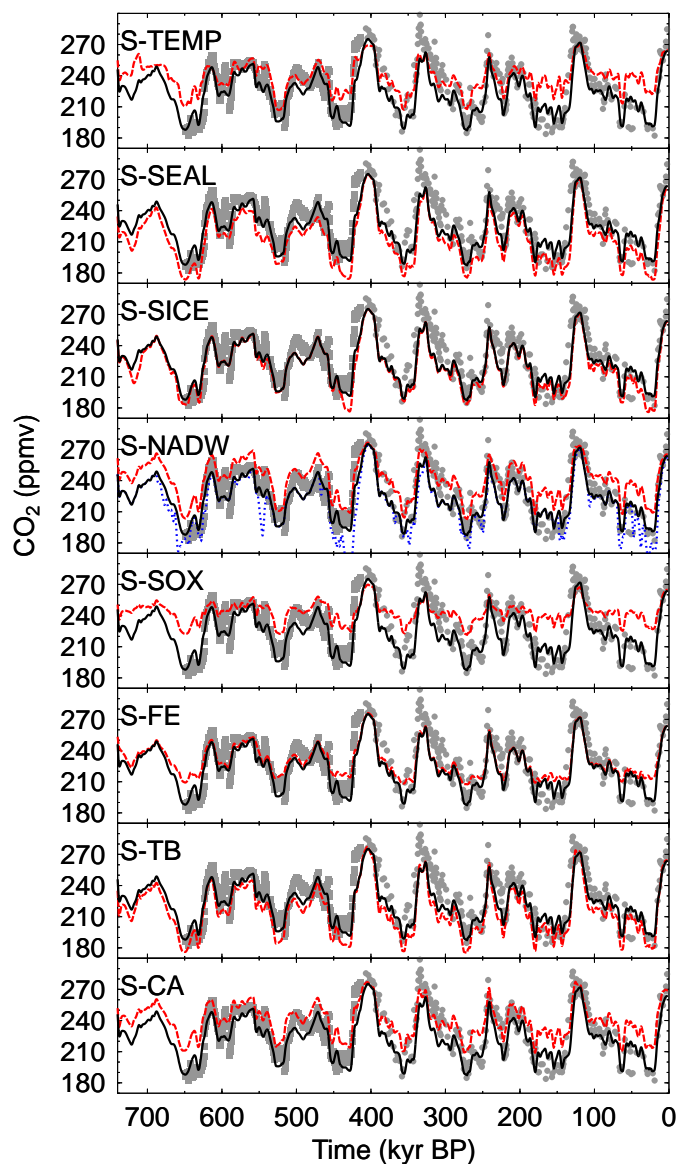


Fig. 8. Analysis of single processes on atmospheric CO₂ in comparison to the CO₂ data (grey markers). All processes (scenario S1.5K, bold black) and all but one process at a time (dash red) were forced externally. Processes depict changes in ocean temperature (S-TEMP), sea level (S-SEAL), sea ice (S-SICE), NADW formation (S-NADW), Southern Ocean vertical mixing (S-SOX), iron fertilisation in the Southern Ocean (S-FE), carbon storage in terrestrial biosphere (S-TB), carbonate compensation (S-CA). Additionally, a scenario with all processes at work and a complete shut-down of NADW formation during all Heinrich events as indicated by IRD in the North Atlantic was simulated (short-dash blue in sub-figure S-NADW). As the inclusion of exchange fluxes between sediment and ocean is converting our modelled carbon cycle to an open system in which total carbon and alkalinity are not conserved anymore a direct comparison between individual simulations becomes difficult due to variations in the overall budgets. All simulation results are shown as 3 kyr running mean.

terminations, drop during glaciations) of up to $30 \mu\text{mol kg}^{-1}$ caused by other processes, which are followed by a relaxation over the following several millenia (Broecker and Peng, 1987). An initial rise in $[\text{CO}_3^{2-}]$ during terminations is caused by the extraction of DIC from the deep waters by any of the other processes operating on the global carbon cycle. This increases the pH of the deep ocean which then moves the equilibrium between $[\text{CO}_2]$, $[\text{HCO}_3^-]$, and

$[\text{CO}_3^{2-}]$ (the three species which add up to DIC) from $[\text{CO}_2]$ towards $[\text{CO}_3^{2-}]$. Dynamics are in the opposite direction during glaciations (input of DIC in the deep ocean; decrease of pH shifts the species equilibrium away from $[\text{CO}_3^{2-}]$). The following relaxation is the response of the sediments to changes in deep ocean $[\text{CO}_3^{2-}]$ by either increased sedimentation (if $[\text{CO}_3^{2-}]$ is increased which shifts the calcite

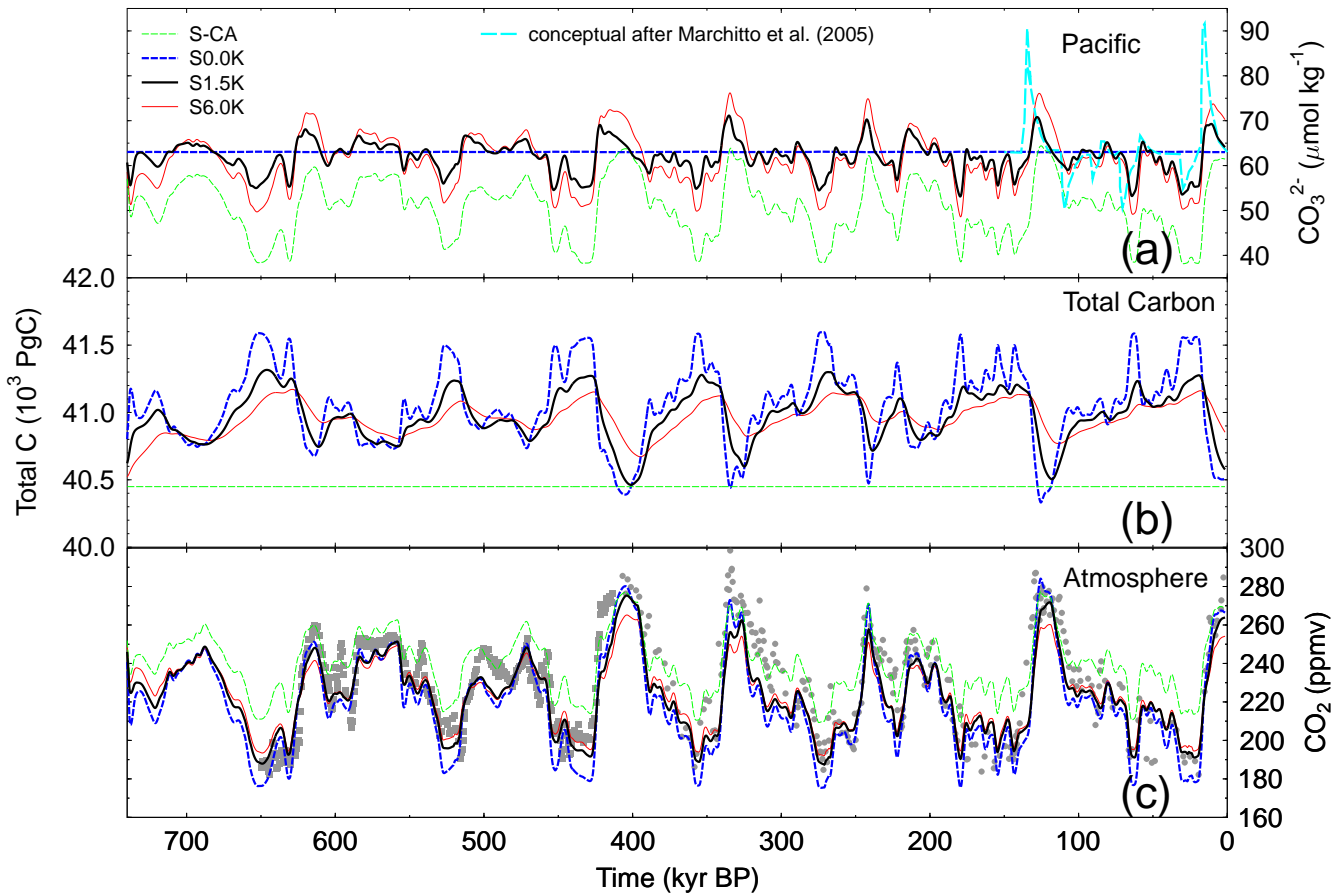


Fig. 9. Carbonate compensation mechanism. Besides the scenarios with different e-folding time of the carbonate compensation (S0.0K, S1.5K, S6.0K) a scenario without CaCO₃ chemistry (S-CA) is shown. Conceptual changes in the deep Pacific CO₃²⁻ concentration expected from measurements (Marchitto et al., 2005) and the understanding of the CaCO₃ compensation are also shown in (a). (a) CO₃²⁻ concentration in the deep Indo-Pacific ocean box. (b) Total carbon of the simulated ocean/atmosphere/biosphere system. (c) Atmospheric CO₂. CO₂ data as described in Fig. 2 as grey markers. All simulation results are shown as 3 kyr running mean.

saturation horizon towards deeper waters) or increased dissolution (if [CO₃²⁻] is decreased which shifts the calcite saturation horizon towards shallower waters) of CaCO₃. Recent measurements on three cores in the equatorial Pacific (Marchitto et al., 2005) support this dynamic, the change in [CO₃²⁻] is of the order of 25–30 μmol kg⁻¹, although the gradients at the beginning of individual events are not as steep as theoretically predicted and the sedimentary response seems to be faster than concluded from process-based models (Fig. 3).

All-together, this means, that a rise in surface waters [CO₂] (similar to a rise in atmospheric CO₂) implies also the extraction of carbon from the deep ocean. This extraction causes increased sedimentation, which is another loss term of carbon. However, due to the ratio of alkalinity:DIC=2:1 in all carbonate fluxes the overall effect of sedimentation is a pH reduction in the deep ocean which again shifts the carbonate system from [CO₃²⁻] towards [CO₂], leading finally

to a further rise in surface [CO₂]. Thus, carbonate compensation is a positive feedback. It always acts as an amplifier to ongoing processes operating on the global carbon cycle.

For this interpretation it has to be kept in mind, that the riverine input of bicarbonate was not explicit formulated, and therefore not allowed to vary over time. Improving this shortcoming together with the use of a process-based sediment model might substantially alter our current understanding of the importance of the CaCO₃ chemistry for atmospheric CO₂.

In conclusion, we have to state that the contribution of the carbonate compensation to the rise in atmospheric CO₂ can only be roughly estimated with our approach. The amplitudes in deep Pacific [CO₃²⁻] in our simulations are about half as large as in observations. A constant deep ocean [CO₃²⁻] caused by instantaneous reacting sediments (S0.0K) is causing a contribution of the carbonate compensation of approximately 35 ppmv (Termination I) which seems to be an upper

estimate. A time-delayed response of the CaCO₃ chemistry reduces this contribution by a factor of two. An ocean carbon cycle model with higher vertical resolution together with a process-based sediment module are needed for a refined quantification of this number.

3.3 Model sensitivity

In the following subsection we will investigate the sensitivity of BICYCLE by the variation of the glacial/interglacial amplitudes of all processes and analyse specific parts of our model in greater detail. These parts (sea ice, ocean circulation, marine biota, terrestrial biosphere) need some in-depth analysis due to the simplicity in which they are embedded in our model.

3.3.1 Variation of the glacial/interglacial strength of individual processes

We investigated the sensitivity of our model to the amplitudes in the different processes contributing to the glacial/interglacial CO₂ rise. We therefore varied their glacial/interglacial amplitudes by up to $\pm 50\%$ from their standards and compared the relative impacts on CO₂ for Termination I (Fig. 10). The sensitivity of the simulated CO₂ to changes in the amplitude of one process is rather linear. Varying the amplitude of a single process by less than 20% would result in less than ~ 7 ppmv deviation in CO₂. We therefore evaluate our model as rather robust to the detailed knowledge of individual processes. This, however, neglects nonlinear effects from combined changes for alternative scenarios in which more than one process is operating with a different glacial/interglacial amplitude.

3.3.2 Sea ice

Our approach proposes a decline of CO₂ by ~ 10 ppmv during terminations contributed by changes in the gas exchange rate through the shrinking of sea ice coverage. This would contradict a previous modelling study (Stephens and Keeling, 2000) which concluded that a nearly full sea ice coverage of the Southern Ocean south of 55° S would reduce CO₂ by 67 ppmv. Although the reliability of this previous study was questioned because of the proposed very high sea ice coverage (Morales-Maqueda and Rahmstorf, 2001) the question remains why our model responses in the opposite direction. It was shown (Archer et al., 2003) that a model response to a fully Southern Ocean sea ice coverage is especially highly model dependent.

In our study the decline in CO₂ during deglaciations is caused by larger gas exchange rate in the North Atlantic Ocean which itself is caused by the decrease in the northern sea ice cover. The preindustrial North Atlantic is a sink for CO₂ while the Southern Ocean is a source, both in our model and if recent gas exchange estimates are corrected for anthropogenic CO₂ (Takahashi et al., 2002; McNeil et al.,

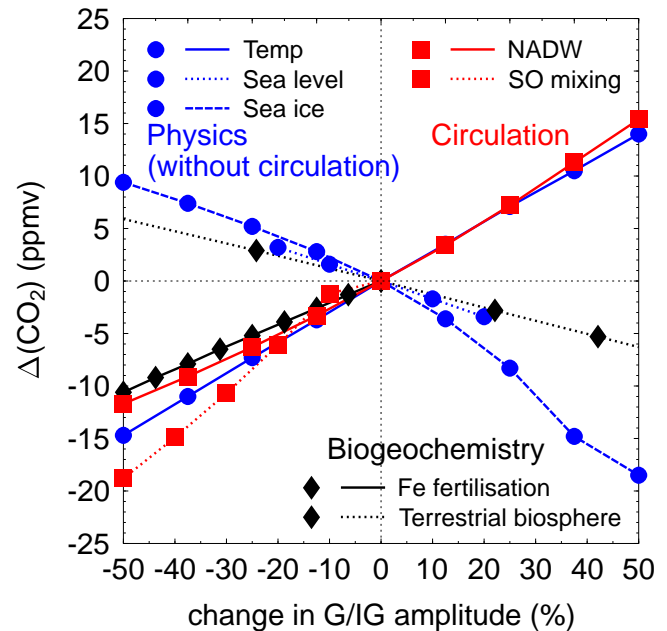


Fig. 10. Sensitivity analysis of the impact of the glacial/interglacial amplitudes of the individual processes on the rise in atmospheric CO₂ during the last glacial/interglacial transition covering Termination I (30–0 kyr). The figure shows the differences in the rise in CO₂ between scenarios (all processes included) with variable amplitude in one process and scenario S1.5K. Processes depict changes in ocean temperature (Temp), sea level, gas-exchange rate through sea ice, NADW formation, Southern Ocean vertical mixing, Fe fertilisation in the Southern Ocean, and carbon storage in terrestrial biosphere. Note, that the carbonate compensation is a response process and cannot be modified in its amplitude. Glacial/interglacial amplitude of sea level change was varied only $\pm 20\%$ due to high reliability of known sea level change. The glacial/interglacial amplitudes of iron (Fe) fertilisation, and Southern Ocean vertical mixing (Southern Ocean mixing) could only be reduced as they were operating on their possible upper limit.

2006). Therefore, reducing gas exchange during glacials in the North is increasing the glacial atmospheric CO₂. The net effect of sea ice coverage in the Southern Ocean is negligible and reaches the magnitude of the North only when the Southern Ocean surface box is nearly fully covered by sea ice (Fig. 11). However, our data based assumption proposes only an average annual glacial sea ice coverage of 30% in our Southern Ocean surface box.

Measurements on gas exchange through sea ice of different temperature come to the conclusions, that gas exchange is not totally prevented by a complete sea ice cover, (Gosink et al., 1976; Semiletov et al., 2004). Furthermore, in our single process analysis we consider only the effect of sea ice on gas exchange rates, while in the previous studies the overall effect of sea ice on both gas exchange and ocean circulation schemes was analysed.

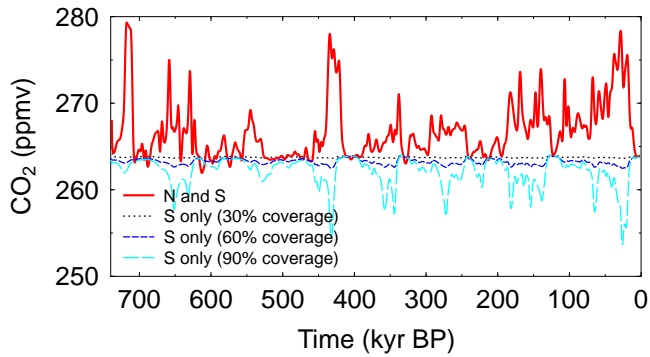


Fig. 11. Northern and southern contributions to the impact of sea ice cover on atmospheric CO₂ in a single processes analysis. In the reference run (N and S) nearly no contribution comes from the Southern Ocean sea ice, which covers 30% of the Southern Ocean surface box area during LGM. Increasing this Southern Ocean sea ice areal cover up to 90% coverage shows opposing trends (reduced CO₂ during glacial times) from the northern contribution (increased CO₂ during glacial times). This Southern Ocean behaviour is in line with previous investigations (Stephens and Keeling, 2000). All simulation results are shown as 3 kyr running mean.

3.3.3 Ocean circulation

In our reference scenario we have chosen to keep NADW formation unchanged during Heinrich events as there are evidences from productivity (Sachs and Anderson, 2005) and sea level (Siddall et al., 2003) reconstructions, that the impact may differ. Here, we estimate the maximum impact through a complete shut-down of NADW formation during Heinrich events identified by ice rafted debris (IRD) in the North Atlantic sediment record ODP980 measured on the same core than two other paleo records used already in our study (North Atlantic SST and benthic $\delta^{18}\text{O}$) (McManus et al., 1999; Wright and Flower, 2002). IRD in percentage of sediment grains larger than 150 μm (relative IRD) is a proxy for the occurrence of Heinrich events (Heinrich, 1988). We used the relative strength $\text{IRD}_H=10\%$ as threshold indicating large iceberg and thus freshwater discharges occurring in the North Atlantic which result in a complete shut-down of the NADW formation during glacial times in our model. This threshold was derived from the analysis of IRD and known Heinrich events during the last glacial cycle (Heinrich, 1988). During two time intervals relative IRD data were missing in ODP980 (740–700 and 543–500 kyr BP). The absolute IRD record (lithics/g) spanned our whole simulation period (Wright and Flower, 2002) and showed no major excursions in the incomplete periods of the relative IRD record apart from one large peak during the period 740–700 kyr BP. However, this absolute record is unsuitable for the predictions of Heinrich events as known events occurring during the last glacial cycle (Heinrich, 1988) would have been overestimated. IRD in a second core approximately 1000 km apart (ODP984) shows

similar features during 500–740 kyr BP (Wright and Flower, 2002) suggesting an at least regional distribution of the IRD signals measured in ODP980 and the changes in freshwater discharge indicated by them.

A shut-down of the NADW formation occurring during the Heinrich events, which were identified by the relative IRD record, reduces atmospheric CO₂ during glacial conditions by about 10–20 ppmv (Fig. 8). Only a Heinrich event around 550 kyr BP happening during intermediate climate conditions and those events in the glacial maximum preceding Termination V (420 kyr BP) lead to drops in CO₂ by 30–40 ppmv. The selection criteria for Heinrich events ($\text{IRD}_H=10\%$) was varied in a sensitivity study (Fig. 12b), and showed rather unchanged response of CO₂ for a threshold increase by a factor of two, and an extension of Heinrich events if IRD_H was lowered.

The impacts of the threshold $\delta^{18}\text{O}_{\text{NADW}}$ in ODP980 which indicates a switch from glacial to interglacial circulation patterns in the Atlantic Ocean (strength of NADW formation) was also tested. During interglacial times this strength in NADW depends to a certain extent on the chosen threshold (Fig. 12a). During warm periods around 200, 570, 610, and 690 kyr BP the Atlantic THC is only switching into its interglacial mode (16 Sv of NADW formation) and leads to a rise in CO₂ by about 10 ppmv, when the threshold $\delta^{18}\text{O}_{\text{NADW}}$ is increased. This implies that in our standard scenarios the NADW stayed in its glacial mode during these times. In other words, the Atlantic THC stayed constant over time in its glacial mode before MIS 11 (740–420 kyr BP) and would switch only to its interglacial mode in the pre-Vostok period if a slightly colder temperature threshold is assumed (higher $\delta^{18}\text{O}_{\text{NADW}}$) than in the standard case.

For the understanding of the consequences of a reduced glacial ocean circulation through either a (partly) shutdown of the Atlantic THC or reduced Southern Ocean vertical mixing one has to keep in mind that our analysis with the BICYCLE model covers only the direct effects of a reduced water transport on the dissolved chemical species (DIC, alkalinity, nutrients). In more sophisticated models changes in ocean circulation lead also to changes in the temperature, and salinity. Temperature and salinity are prescribed externally within BICYCLE. A reduced strength of the NADW formation would lead to a temperature drop in the North Atlantic which is spread over large parts of Eurasia and a rise in Southern Ocean temperatures following the concept of a bipolar seesaw (e.g. Stocker and Johnsen, 2003). The direct effect of these temperature anomalies on CO₂ would lead to an outgassing of CO₂ in the Southern Ocean and a higher solubility and a down draw of CO₂ in the north Atlantic. As a follow-up effect the sea ice cover in the North would increase while that in the South would shrink. Because of the opposite effects of sea ice on atmospheric CO₂ in both hemispheres (see above) the northern sea ice expansion and the southern decline would both lead to a rise in atmospheric CO₂ during a reduced Atlantic THC. Additionally, the millennial scale

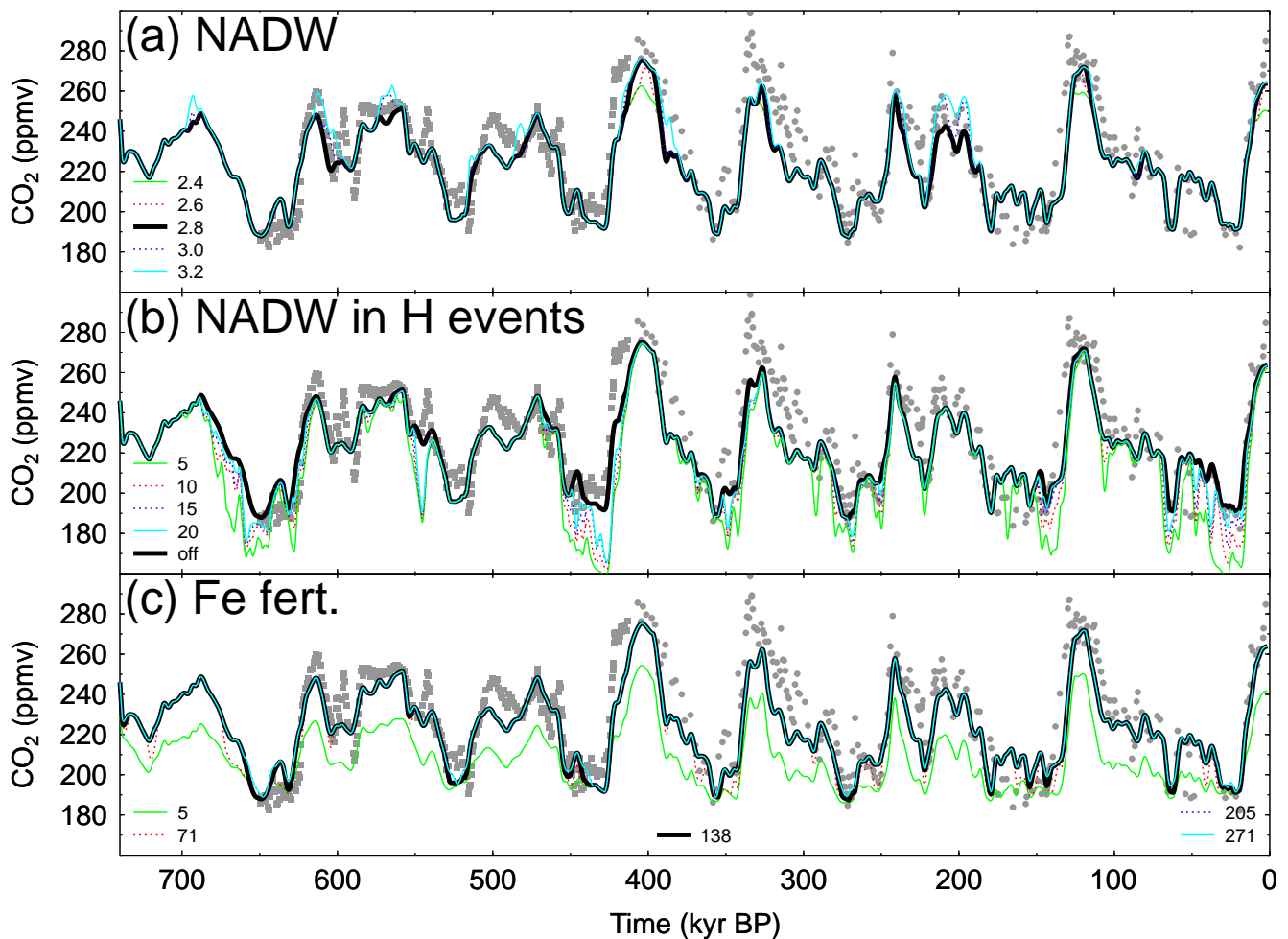


Fig. 12. Variation of fixed threshold values used during simulations. Simulation results were shown as 3 kyr running mean. Bold depicts always the standard simulation S1.5K using the standard values, data (grey markers) as described in Fig. 2. (a): Varying the threshold $\delta^{18}\text{O}_{\text{NADW}}$ in ODP980 which indicates changes in the strength in the NADW formation ($\delta^{18}\text{O}_{\text{NADW}}=2.4, 2.6, 2.8, 3.0, 3.2\text{‰}$). (b): Varying the threshold in IRD as the indicator for Heinrich events measured in ODP980 ($\text{IRD}_{\text{H}}=5, 10, 15, 20\%$). Note, that in our standard scenario the NADW formation during identified Heinrich events is not shut-down. (c): Varying the threshold in the atmospheric iron flux as measured in EPICA Dome C which is a proxy for the onset of iron fertilisation in the Southern Ocean ($\text{Fe}_{\text{MB}}=5, 71, 138, 205, 271 \mu\text{g m}^{-2} \text{yr}^{-1}$).

temperature anomalies during Heinrich events would also impact on the terrestrial carbon cycle (Köhler et al., 2005b). During cold periods the treeline in Eurasia would shift southwards, and soil respiration would decrease. In BICYCLE the nutrient distribution is also affected by a change in ocean circulation. But only a reduction in the NADW formation below the glacial strength of 10 Sv causes a decrease in the marine export production due to macro-nutrient depletion and causes a rise in atmospheric CO₂. This change in the marine biota is in line with other studies (Schmittner, 2005). A more detailed investigation of the NADW strength and CO₂ in BICYCLE is found in Köhler et al. (2006).

3.3.4 Marine biota

It was argued recently based on the knowledge gained from open ocean experiments that only 0.5 to 15% of the the glacial/interglacial rise in CO₂ can be caused by iron fertilisation of the marine biota (de Baar et al., 2005). However, their estimate was based on the assumption that the glacial aeolian iron input into the Antarctic region was 11-fold its modern flux, while recent data from EPICA Dome C find a 25- to 34-fold increase in iron fluxes from interglacial to glacial periods (Gaspari et al., 2006; Wolff et al., 2006). In our simulation results, which use the higher iron flux changes measured in Antarctic ice cores the contribution of this process to the CO₂ rise covers approximately 25% of the observed signal. This is within the range covered by the iron

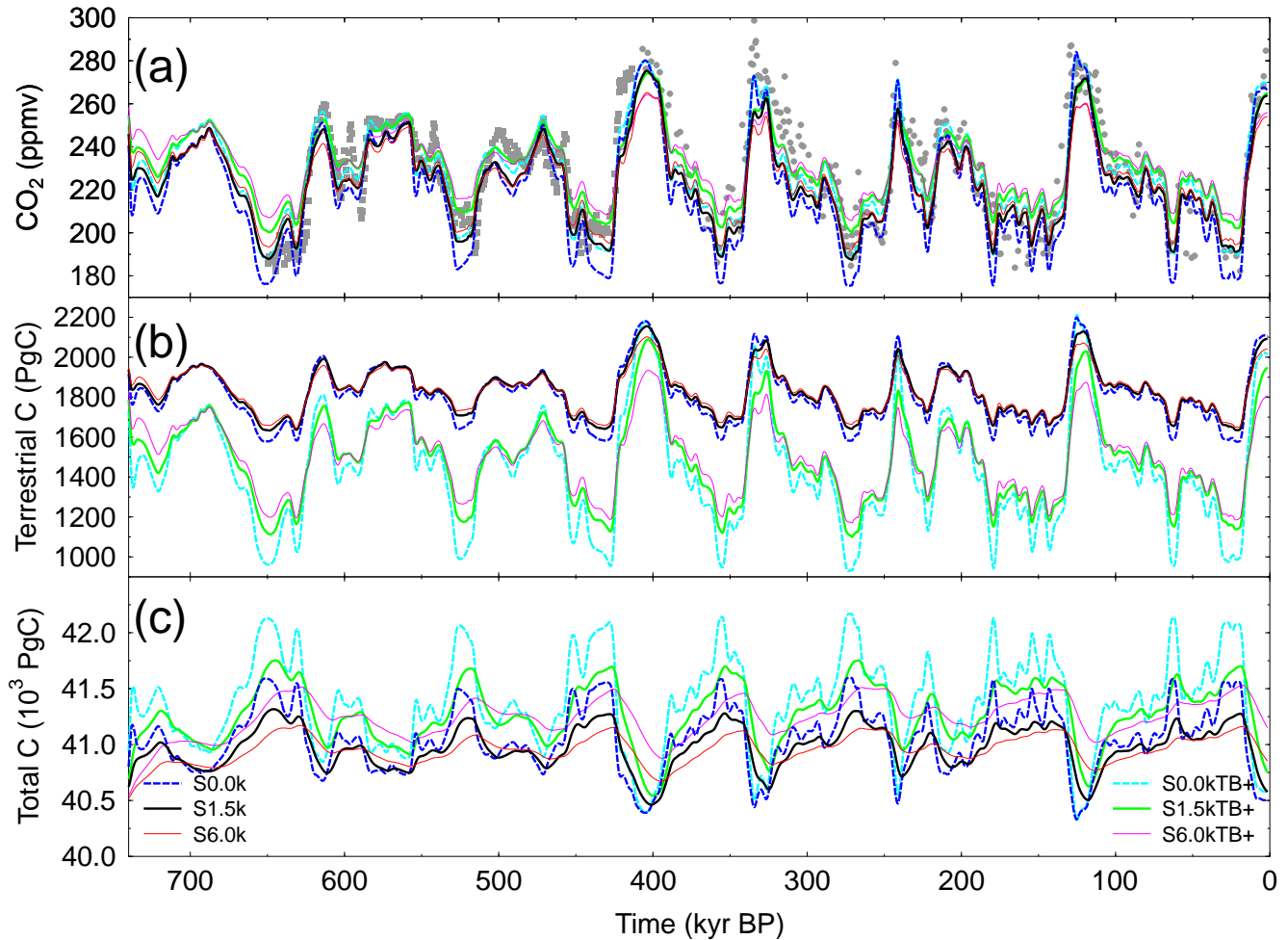


Fig. 13. Additionally to the simulation S0.0K, S1.5K, S6.0K an alternative pathway of terrestrial biosphere regrowth was considered with greater climate and CO₂ dependency leading to higher glacial/interglacial amplitudes in the terrestrial carbon stocks (S0.0kTB+, S1.5kTB+, S6.0kTB+). Different e-folding time of the calcite compensation as given in the scenario names. **(a):** Atmospheric CO₂, data (grey markers) as described in Fig. 2. **(b):** Terrestrial carbon storage. **(c):** Total carbon storage in the atmosphere/ocean/biosphere system. All simulation results are shown as 3 kyr running mean.

fertilisation experiments. Additional to the data evidences for an enhanced glacial marine biology as reviewed previously (Köhler et al., 2005a) new data of extensive phytoplankton blooms in the Atlantic sector of the glacial Southern Ocean were published recently (Abelmann et al., 2006), giving further support for our assumptions.

The impact of Southern Ocean iron fertilisation on CO₂ was also a threshold-dependent process. Changes in simulated CO₂ occur for a two fold reduction of the threshold during times of high iron flux fluctuations, e.g. around 150–180 kyr BP. Simulated atmospheric CO₂ varied significantly (>20 ppmv) if the threshold in the EPICA Dome C iron flux on which the marine export production depends is reduced by one order of magnitude (Fig. 12c). This would imply that the marine biota in the Southern Ocean is nearly never iron limited and global export production reduces at-

mospheric CO₂ throughout most of the simulation period. The threshold approach neglects details in the dynamics of the different iron proxies for full glacial conditions and is partly responsible for the similar responses of our model to the use of the three different iron proxies.

3.3.5 Terrestrial biosphere

To cover the estimated range in the glacial/interglacial rise in terrestrial carbon storage of 300–1100 PgC (Köhler and Fischer, 2004) an alternative pathway with increased sensitivity of the terrestrial biosphere to CO₂ and climate change was considered. Terrestrial carbon storage varies during Termination I by 400 to 500 PgC in the previous scenarios (S0.0K, S1.5K, S6.0K) and 800–1100 PgC alternatively (S0.0kTB+, S1.5kTB+, S6.0kTB+) (Fig. 13b). The parameterisation of

the sensitivity of the terrestrial module on climate and CO₂ is the same within the two sets of experiments. The existing difference in the amplitudes within a set of simulations is caused by the internal feedback of the CO₂ dependent terrestrial NPP (CO₂ fertilisation). The change in the amplitude in terrestrial carbon storage leads also to different CaCO₃ fluxes between sediment and deep ocean and thus to different fluctuations in the overall carbon budget. While the change in the total carbon of the simulated ocean/atmosphere/biosphere system is 1000, 700, and 350 PgC in S0.0K, S1.5K and S6.0K, respectively, this amplitude is increased to 1700, 1000, and 500 PgC in S0.0KTB+, S1.5KTB+ and S6.0KTB+ (Fig. 13c). In S1.5KTB+ and S6.0KTB+ the total C content at $t=0$ kyr BP is 250 and 500 PgC higher than in steady state simulations for this climate period. This offset in the total C budget between transient simulations and preindustrial steady state makes the upper end of the proposed range in the variation of the terrestrial carbon content very unlikely. As overall effect glacial atmospheric CO₂ is about 15 ppmv higher in the STB+ scenarios than in the corresponding simulations with lower terrestrial variability (Fig. 13a).

4 Discussion and conclusions

In this study we simulate low frequency changes in the carbon cycle during the late Pleistocene. Our standard scenarios match observed atmospheric CO₂ during the last 650 kyr rather well ($r^2 \sim 0.75$). The novelty of our approach is the fact that our interpretation how the global carbon cycle including its isotopes is operating during Termination I seems to be sufficient to interpret the variations in atmospheric CO₂ not only during the regular variations observed in the Vostok ice core but also to simulate smaller glacial/interglacial amplitudes prior to Termination V. The application of our model on these long timescales is a confirmation that our assumptions made for and our interpretation gained from the simulation of the carbon cycle during Termination I (Köhler et al., 2005a) are not restricted to this very narrow time window, but are of general nature. The time-delayed response of the carbonate compensation is an important detail of the CaCO₃ chemistry which was not considered in earlier applications of this model. The e-folding time τ of the relaxation of any perturbation of the deep ocean [CO₃²⁻] estimated from data and models is still large, however, the consequences are even with a moderate response time ($\tau=1.5$ kyr) that the carbon cycle in our model never reaches an equilibrium within the last 740 kyr; the total carbon budget is constantly varying due to sedimentation or dissolution. Carbonate compensation with moderate response time (1.5 kyr) contributes about 15 ppmv to the rise of CO₂ during the last five terminations. This is of the order suggested by Joos et al. (2004) during the Holocene as a consequence of the reorganisation of the carbon cycle over Termination I. It is about half of the amount suggested by our previous study (Köhler et al., 2005a), in

which we alternatively prescribed the changes in the lysocline as additional boundary condition. These lysocline variations, however, are less well known over the whole 740 kyr period for the different ocean basins (Farrell and Prell, 1989) and the interpretation of available data is highly discussed (Archer, 1991). The previous approach of a variable lysocline leads to results similar to those of the scenario with instantaneously responding sediments (S0.0K). The missing response time in this approach was therefore a reason to revise and update our model here.

The missing temporal variability of the riverine input of bicarbonate and its subsequent response by the carbonate compensation might be one of the main simplifications of our study. The input of HCO₃⁻ through rivers is estimated to vary on glacial/interglacial timescale by about 25% (Jones et al., 2002; Munhoven, 2002). This reduced interglacial riverine input leads to a rise of atmospheric CO₂ of the order of 10 ppmv, however, uncertainties in both the variability of the input fluxes itself and the response of the carbon cycle are with about 100% large.

There are several hypothesis on possible changes in the carbon cycle found in the literature, which we did not follow up here for various reasons, because they are either too complex to be followed in detail with our model (silicic acid leakage hypothesis), because of recent evidences arguing against them (rain ratio hypothesis), or because we expect only small contributions to the change in CO₂ (North Pacific biology). They are discussed in greater detail in Köhler et al. (2005a). The potential of a change in the rain ratio of organic to inorganic marine export production, for example, is one theory (Archer and Maier-Reimer, 1994; Klaas and Archer, 2002; Ridgwell, 2003a), whose impact on CO₂ is limited to less than 15 ppmv in BICYCLE. The silicic acid leakage hypothesis (Brzezinski et al., 2002; Matsumoto et al., 2002) involves shifts in phytoplankton communities and operates via a combination of iron fertilisation in the Southern Ocean and local changes in the the rain ratio. Other HNLC regions of the world ocean apart from the Southern Ocean have also the potential for an enhanced glacial export production, although with less capacity for atmospheric CO₂. One of these prominent regions is the North Pacific where a higher glacial export production might result in a decrease in CO₂ of up to 8 ppmv (Röthlisberger et al., 2004). A recent interpretation of proxy data (Jaccard et al., 2005) makes this region also a candidate for a highly stratified water column in glacial times. This physical effect might be even more important for CO₂ than the change in the biology.

Our results are further supported by reconstructed pH in the equatorial Atlantic surface waters, which are based on $\delta^{11}\text{B}$ measurements from planktic foraminifers (Hönisch and Hemming, 2005). As we calculate the whole carbonate system in our model, we are able to compare our simulated pH variations in the surface water box of the equatorial Atlantic with these measurements (Fig. 14). Although the data set is sparse our model predicts a similar glacial/interglacial

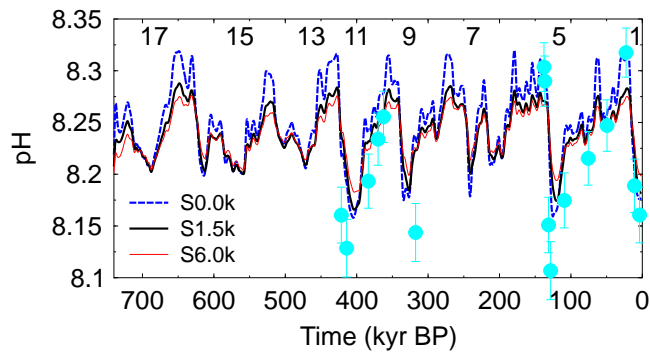


Fig. 14. Comparison of simulated pH in the equatorial Atlantic surface box with pH reconstruction (circles) based on boron isotopes $\delta^{11}\text{B}$ measured in planktic foraminifers (Hönisch and Hemming, 2005). Simulation results are shown as 3 kyr running mean. Numbers denote marine isotope stages during interglacial periods.

amplitude of up to 0.15 pH units (scenario S0.0K; less than 0.10 pH units in S1.5K and S6.0K) in this area, although minima during interglacial periods are smaller in the data than in the model.

These simulation results are an in-depth description of our contribution to the “EPICA challenge” (Wolff et al., 2004, 2005). The other seven entries to the “EPICA challenge” (Wolff et al., 2005) were either based on a conceptual modelling approach (Paillard and Parrenin, 2004) or on different correlation functions of the two EPICA Dome C records (dust, δD) and others paleo-climatic archives. Thus, they all tested different hypotheses, but were per se unable to validate their hypothesis by the comparison of other variables of the carbon cycle with additional reconstructions. Nevertheless, all other approaches using existing Antarctic temperature proxies and simple regression functions were able to predict CO₂ with similar high accuracy (Wolff et al., 2005). Can we understand this coupling of atmospheric CO₂ and Antarctic/Southern Ocean temperature from our process-based modelling approach? SST of the Southern Ocean itself (which is a function of EPICA Dome C δD) is according to our model responsible for half of the rise in CO₂ caused by ocean temperature, which would be ~ 15 ppmv during Termination I. Changes in sea ice cover and Southern Ocean vertical mixing are in BICYCLE functions of Southern Ocean SST and thus of EPICA Dome C δD , causing 0 ppmv and 35 ppmv, respectively. Furthermore, CaCO₃ compensation as amplifying process will contribute about 5–10 ppmv. Summarising, we are able to explain a rise in CO₂ of 55–60 ppmv during Termination I only by direct and indirect effects of Southern Ocean temperature changes and thus by the evolution of the EPICA Dome C δD record. However, these are incomplete solutions, because other important changes in the carbon cycle are known to have happened, such as changing concentration of DIC due to sea level variations or changing carbon storage on land which would both operate in the opposite direction.

To our knowledge, there exist so far two transient modelling approaches which try to explain the variability of atmospheric CO₂ during the late Pleistocene both using conceptual models (Gildor et al., 2002; Paillard and Parrenin, 2004) and concentrate on changes in ocean physics. These two approaches differ widely, one (Gildor et al., 2002) being purely theoretically and trying to explain the typical amplitude and seesaw shape of CO₂ observed in Vostok, while the other (Paillard and Parrenin, 2004) is forced by insolation over the last 1000 kyr. However, both pinpoint reduced glacial vertical mixing in the Southern Ocean as one mechanism which contributes significantly to the glacial/interglacial rise in CO₂. While we here support the importance of changes in Southern Ocean vertical mixing, we also want to point out that especially those processes which modify the overall budgets of DIC and alkalinity in the ocean need consideration (Archer et al., 1997) and a restricted view onto the ocean/atmosphere carbonate system only is of limited validity for a complete understanding of the observed changes in the carbon cycle as recorded in the ice cores.

The chosen model design, that Southern Ocean vertical mixing is a function of Southern Ocean temperature and thus of EPICA Dome C δD , might be questioned. It was motivated by the observed vertical and temporal gradient in $\delta^{13}\text{C}$ in the Southern Ocean sediment cores (Hodell et al., 2003). It turns out that this process is the most important one for atmospheric CO₂ variability. As a consequence this process alone together with its amplification through CaCO₃ compensation can explain 40 ppmv of the rise in CO₂ during Termination I. To support this assumption we argued previously (Köhler et al., 2005a) with additional evidences from nutrient reconstructions (François et al., 1997) and the salinity-driven stratification of the glacial ocean (Adkins et al., 2002). Further support came from the two conceptual models mentioned earlier (Gildor et al., 2002; Paillard and Parrenin, 2004) and a box model study which investigates the role of Southern Ocean mixing and upwelling on CO₂ (Watson and Naveira-Garabato, 2006). In the meantime, another physically based hypothesis was added to the scenarios which propose a glacial stratified Southern Ocean. Toggweiler et al. (2006) hypothesised that a northward shift in the westerly winds during glacial climate would prevent wind-driven upwelling in the Southern Ocean. Their carbon cycle response to this change in ocean ventilation is a glacial decrease in atmospheric CO₂ of 35 ppmv, very similar to our results.

The various simplification of the carbon cycle in terms of spatial and temporal resolution and the degree to which processes are modelled have to be kept in mind in the interpretation of the results. Furthermore, the detailed response of the carbon cycle differs if omitted feedbacks which would arise from carbon cycle-climate interactions would be considered. The rise in CO₂ leading to enhanced terrestrial photosynthesis is in principle but very simplistically covered within our approach, however, details on the various effects are still matter

of debate (e.g. Bender, 2003; Friedlingstein et al., 2003). The overall effect of temperature variations on soil carbon storage is not yet resolved (Davidson and Janssens, 2006). The feedback loop of climate, dust and CO₂ (Ridgwell and Watson, 2002) is another example for the complexity of the system. Laboratory experiments indicate a CO₂-dependent calcite production rate of marine calcifiers (Riebesell et al., 2000). These are some examples of the complexity of the carbon cycle-climate system, whose detailed investigation is needed for an in-depth understanding. Nevertheless, from our simple approach here the potentials of various globally important processes can be highlighted, and thus the choice of foci for future investigations is possible.

This box model study provides an interpretation of low frequency changes in atmospheric CO₂ during the past 740 kyr based on a carbon cycle box model forced by various paleoclimatic records forward in time. The potential contributions of important physical and biogeochemical processes to CO₂ variability were investigated. As this study is based on a rather simplistic model which highlights also the uncertainties embedded within the approach its results should be understood as an invitation to more complex coupled carbon cycle-climate models to be cross-checked as a whole or in specific parts.

Acknowledgements. This study was performed within RESPIC, a project funded through the German Climate Research Programme DEKLIM (BMBF). R. Bintanja, B. Hönisch, J. Jouzel, V. Masson-Delmotte, J. McManus and U. Siegenthaler kindly provided data sets. We like to thank the EPICA challenge team for the inspiring scientific quest. Thanks to E. Wolff, V. Brovkin, and the three anonymous referees for their helpful comments on the discussion version of this article. This work is a contribution to the European Project for Ice Coring in Antarctica (EPICA), a joint European Science Foundation/European Commission scientific programme, funded by the EU (EPICA-MIS) and by national contributions from Belgium, Denmark, France, Germany, Italy, the Netherlands, Norway, Sweden, Switzerland and the United Kingdom. The main logistic support was provided by IPEV and PNRA (at Dome C) and AWI (at Dronning Maud Land). This is EPICA publication no. 145.

Edited by: V. Brovkin

References

- Abelmann, A., Gersonde, R., Cortese, G., Kuhn, G., and Smetacek, V.: Extensive phytoplankton blooms in the Atlantic sector of the glacial Southern Ocean, *Paleoceanography*, 21, PA1013; doi:10.1029/2005PA001199, 2006.
- Adkins, J. F., McIntyre, K., and Schrag, D. P.: The salinity, temperature, and $\delta^{18}\text{O}$ of the glacial deep ocean, *Science*, 298, 1769–1773, 2002.
- Archer, D. and Maier-Reimer, E.: Effect of deep-sea sedimentary calcite preservation on atmospheric CO₂ concentration, *Nature*, 367, 260–263, 1994.
- Archer, D., Kheshgi, H., and Maier-Reimer, E.: Multiple timescales for neutralization of fossil fuel CO₂, *Geophys. Res. Lett.*, 24, 405–408, 1997.
- Archer, D., Kheshgi, H., and Maier-Reimer, E.: Dynamics of fossil fuel neutralization by marine CaCO₃, *Global Biogeochem. Cycles*, 12, 259–276, 1998.
- Archer, D., Winguth, A., Lea, D., and Mahowald, N.: What caused the glacial/interglacial atmospheric $p\text{CO}_2$ cycles?, *Rev. Geophys.*, 38, 159–189, 2000.
- Archer, D. E.: Equatorial Pacific calcite preservation cycles: production or dissolution?, *Paleoceanography*, 6, 561–571, 1991.
- Archer, D. E.: An atlas of the distribution of calcium carbonate in sediments of the deep sea, *Global Biogeochem. Cycles*, 10, 159–174, 1996.
- Archer, D. E., Martin, P. A., Milovich, J., Brovkin, V., Plattner, G.-K., and Ashendel, C.: Model sensitivity in the effect of Antarctic sea ice and stratification on atmospheric $p\text{CO}_2$, *Paleoceanography*, 18, 1012, doi:10.1029/2002PA000760, 2003.
- Barnola, J. M., Raynaud, D., Korotkevich, Y. S., and Lorius, C.: Vostok ice core provides 160 000-year record of atmospheric CO₂, *Nature*, 329, 408–414, 1987.
- Bender, M.: Climate-biosphere interactions on glacial-interglacial timescales, *Global Biogeochem. Cycles*, 17, 1082, doi:10.1029/GB001932, 2003.
- Bintanja, R., van der Wal, R., and Oerlemans, J.: Modelled atmospheric temperatures and global sea levels over the past million years, *Nature*, 437, 125–128; doi:10.1038/nature03975, 2005.
- Broecker, W., Barker, S., Clark, E., Hajdas, I., Bonani, G., and Stott, L.: Ventilation of the glacial deep Pacific Ocean, *Science*, 306, 1169–1172, 2004.
- Broecker, W. S. and Peng, T.-H.: The role of CaCO₃ compensation in the glacial to interglacial atmospheric CO₂ change, *Global Biogeochem. Cycles*, 1, 15–29, 1987.
- Brook, E. J.: Tiny bubbles tell all, *Science*, 310, 1285–1287, doi:10.1126/science.11211535, 2005.
- Brzezinski, M. A., Pride, C. J., Franck, V. M., Sigman, D. M., Matsumoto, J. L. S. K., Gruber, N., Rau, G. H., and Coale, K. H.: A switch from Si(OH)₄ to NO₃⁻ depletion in the glacial Southern Ocean, *Geophys. Res. Lett.*, 29, 1564, doi:10.1029/2001GL014349, 2002.
- Cavaliere, D. J., Gloersen, P., Parkinson, C. L., Comiso, J. C., and Zwally, H. J.: Observed hemispheric asymmetry in global sea ice changes, *Science*, 278, 1104–1106, 1997.
- Crosta, X., Pichon, J.-J., and Burckle, L. H.: Application of modern analog technique to marine Antarctic diatoms: Reconstruction of maximum sea-ice extent at the Last Glacial Maximum, *Paleoceanography*, 13, 284–297, 1998a.
- Crosta, X., Pichon, J.-J., and Burckle, L. H.: Reappraisal of Antarctic seasonal sea-ice extent at the Last Glacial Maximum, *Geophys. Res. Lett.*, 14, 2703–2706, 1998b.
- Davidson, E. A. and Janssens, I. A.: Temperature sensitivity of soil carbon decomposition and feedbacks to climate change, *Nature*, 440, 165–173, doi:10.1038/nature04514, 2006.
- de Baar, H. J. W., Boyd, P. W., Coale, K. H., Landry, M. R., Tsuda, A., Assmy, P., Bakker, D. C. E., Bozec, Y., Barber, R. T., Brzezinski, M. A., Buesseler, K. O., Boyé, M., Croot, P. L., Gervais, F., Gorbunov, M. Y., Harrison, P. J., Hiscock, W. T., Laan, P., Lancelot, C., Law, C. S., Lavoie, M., Marchetti, A., Millero, F. J., Nishioka, J., Nojiri, Y., van Oijen, T., Riebesell, D., and Smetacek, V.: The Southern Ocean CO₂ Experiment (SOCEX-2): A synthesis of results, *Global Biogeochem. Cycles*, 17, 1082, doi:10.1029/GB001932, 2003.

- sell, U., Rijkenberg, M. J. A., Saito, H., Takeda, S., Timmermans, K. R., Veldhuis, M. J. W., Waite, A. M., and Wong, C.-S.: Synthesis of iron fertilization experiments: From the Iron Age in the Age of Enlightenment, *J. Geophys. Res.*, 110, C09S16, doi:10.1029/2004JC002601, 2005.
- EPICA-community-members: Eight glacial cycles from an Antarctic ice core, *Nature*, 429, 623–628, 2004.
- Farrell, J. W. and Prell, W. L.: Climate change and CaCO₃ preservation: An 800,000 year bathymetric reconstruction from the central equatorial Pacific Ocean, *Paleoceanography*, 4, 447–466, 1989.
- Fischer, H., Wahlen, M., Smith, J., Mastroianni, D., and Deck, B.: Ice core records of atmospheric CO₂ around the last three glacial terminations, *Science*, 283, 1712–1714, 1999.
- Flower, B. P., Oppo, D. W., McManus, J. F., Venz, K. A., Hodell, D. A., and Cullen, J. L.: North Atlantic intermediate to deep water circulation and chemical stratification during the past 1 Myr, *Paleoceanography*, 15, 388–403, 2000.
- François, R., Altabet, M. A., Yu, E.-F., Sigman, D. M., Pacon, M. P., Frankl, M., Bohrmann, G., Bareille, G., and Labeyrie, L. D.: Contribution of Southern Ocean surface-water stratification to low atmospheric CO₂ concentrations during the last glacial period, *Nature*, 389, 929–935, 1997.
- Friedlingstein, P., Dufresne, J.-L., Cox, P. M., and Rayner, P.: How positive is the feedback between climate change and the carbon cycle?, *Tellus*, 55B, 692–700, 2003.
- Ganachaud, A. and Wunsch, C.: Improved estimates of global ocean circulation, heat transport and mixing from hydrographic data, *Nature*, 408, 453–457, 2000.
- Gaspari, V., Barbante, C., Cozzi, G., Cescon, P., Boutron, C. F., Gabrielli, P., Capodaglio, G., Ferrari, C., Petit, J. R., and Delmonte, B.: Atmospheric iron fluxes over the last deglaciation: Climatic implications, *Geophys. Res. Lett.*, 33, L03704; doi:10.1029/2005GL024352, 2006.
- Gersonde, R., Crosta, X., Abelmann, A., and Armand, L.: Sea-surface temperature and sea ice distribution of the Southern Ocean at the EPILOG Last Glacial Maximum – a circum-Antarctic view based on siliceous microfossil records, *Quat. Sci. Rev.*, 24, 869–896, 2005.
- Gildor, H., Tziperman, E., and Toggweiler, J. R.: Sea ice switch mechanism and glacial-interglacial CO₂ variations, *Global Biogeochem. Cycles*, 16, 1032, doi:10.1029/2001GB001446, 2002.
- Gnanadesikan, A., Slater, R. D., Gruber, N., and Sarmiento, J. L.: Oceanic vertical exchange and new production: a comparison between models and observations, *Deep-Sea Res. II*, 49, 363–401, 2002.
- Gosink, T. A., Pearson, J. G., and Kelley, J. J.: Gas movement through sea ice, *Nature*, 263, 41–42, 1976.
- Heinrich, H.: Origin and consequences of cyclic ice rafting in the northeast Atlantic ocean during the past 130,000 years, *Quat. Res.*, 29, 142–152, 1988.
- Hodell, D. A., Venz, K. A., Charles, C. D., and Ninnemann, U. S.: Pleistocene vertical carbon isotope and carbonate gradients in the South Atlantic sector of the Southern Ocean, *Geochemistry, Geophysics, Geosystems*, 4, 1004, doi:10.1029/2002GC000367, 2003.
- Hönisch, B. and Hemming, N. G.: Surface ocean pH response to variations in pCO₂ through two full glacial cycles, *Earth Planet. Sci. Lett.*, 236, 305–314, 2005.
- Jaccard, S. L., Haug, G. H., Sigman, D. M., Pedersen, T. F., Thierstein, H. R., and Röhl, U.: Glacial/interglacial changes in subarctic North Pacific stratification, *Science*, 308, 1003–1006, 2005.
- Jin, X., Gruber, N., Dunne, J. P., Sarmiento, J. L., and Armstrong, R. A.: Diagnosing the contribution of phytoplankton functional groups to the production and export of particulate organic carbon, CaCO₃, and opal from global nutrient and alkalinity distributions, *Global Biogeochem. Cycles*, 20, GB2015; doi:10.1029/2005GB002532, 2006.
- Jones, I. W., Munhoven, G., Tranter, M., Huybrechts, P., and Sharp, M. J.: Modelled glacial and non-glacial HCO₃⁻, Si and Ge fluxes since the LGM: little potential for impact on atmospheric CO₂ concentrations and a potential proxy of continental chemical erosion, the marine Ge/Si ratio, *Global and Planetary Change*, 33, 139–153, 2002.
- Joos, F., Gerber, S., Prentice, I. C., Otto-Bliesner, B. L., and Valdes, P. J.: Transient simulations of Holocene atmospheric carbon dioxide and terrestrial carbon since the Last Glacial Maximum, *Global Biogeochem. Cycles*, 18, GB2002, doi:10.1029/2003GB002156, 2004.
- Jouzel, J., Lorius, C., Petit, J. R., Genthon, C., Barkov, N. I., Kotlyakov, V. M., and Petrov, V. M.: Vostok ice core: a continuous isotope temperature record over the last climate cycle (160 000 years), *Nature*, 329, 403–408, 1987.
- Jouzel, J., Vimeux, F., Caillon, N., Delaygue, G., Hoffmann, G., Masson-Delmotte, V., and Parrenin, F.: Magnitude of isotopics/temperature scaling for interpretation of central Antarctic ice cores, *J. Geophys. Res.*, 108, 4361, doi:10.1029/2002JD002677, 2003.
- Kawamura, K., Nakazawa, T., Aoki, S., Sugawara, S., Fujii, Y., and Watanabe, O.: Atmospheric CO₂ variations over the last three glacial-interglacial climatic cycles deduced from the Dome Fuji deep ice core, Antarctica using a wet extraction technique, *Tellus*, 55B, 126–137, 2003.
- Klaas, C. and Archer, D. E.: Association of sinking organic matter with various types of mineral ballast in the deep sea: Implications for the rain ratio, *Global Biogeochem. Cycles*, 16, 1116, doi:10.1029/2001GB001765, 2002.
- Knorr, G. and Lohmann, G.: Southern Ocean origin for the resumption of Atlantic thermohaline circulation during deglaciation, *Nature*, 424, 532–536, 2003.
- Köhler, P. and Fischer, H.: Simulating changes in the terrestrial biosphere during the last glacial/interglacial transition, *Global and Planetary Change*, 43, 33–55, doi:10.1016/j.gloplacha.2004.02.005, 2004.
- Köhler, P., Fischer, H., Munhoven, G., and Zeebe, R. E.: Quantitative interpretation of atmospheric carbon records over the last glacial termination, *Global Biogeochem. Cycles*, 19, GB4020, doi:10.1029/2004GB002345, 2005a.
- Köhler, P., Joos, F., Gerber, S., and Knutti, R.: Simulated changes in vegetation distribution, land carbon storage, and atmospheric CO₂ in response to a collapse of the North Atlantic thermohaline circulation, *Clim. Dyn.*, 25, 689–708, doi:10.1007/s00382-005-0058-8, 2005b.
- Köhler, P., Muscheler, R., and Fischer, H.: A model-based interpretation of low frequency changes in the carbon cycle during the last 120 kyr and its implications for the reconstruction of atmospheric $\Delta^{14}\text{C}$, *Geochemistry, Geophysics, Geosystems*, in press, doi:10.1029/2005GC001228, 2006.

- Kutzbach, J., Gallimore, R., Harrison, S., Behling, P., Selin, R., and Laarif, F.: Climate and biome simulations for the past 21 000 years, *Quat. Sci. Rev.*, 17, 473–506, 1998.
- Labeyrie, L. D., Duplessy, J. C., and Blanc, P. L.: Variations in mode of formation and temperature of oceanic deep waters over the past 125 000 years, *Nature*, 327, 477–482, 1987.
- Legrand, M.: Chemistry of Antarctic snow and ice, *J. Phys.*, 48/C1, 77–86, 1987.
- Lisiecki, L. E. and Raymo, M. E.: A Pliocene-Pleistocene stack of 57 globally distributed benthic $\delta^{18}\text{O}$ records, *Paleoceanography*, 20, PA1003, doi:10.1029/2004PA001071, 2005.
- Marchitto, T. M., Lynch-Stieglitz, J., and Hemming, S. R.: Deep Pacific CaCO₃ compensation and glacial-interglacial atmospheric CO₂, *Earth Planet. Sci. Lett.*, 231, 317–336, 2005.
- Martin, J. H.: Glacial-interglacial CO₂ change: the iron hypothesis, *Paleoceanography*, 5, 1–13, 1990.
- Matsumoto, K., Sarmiento, J. L., and Brzezinski, M. A.: Silicic acid leakage from the Southern Ocean: a possible explanation for glacial atmospheric $p\text{CO}_2$, *Global Biogeochem. Cycles*, 16, 1031, doi:10.1029/2001GB001442, 2002.
- McManus, J. F., Oppo, D. W., and Cullen, J. L.: A 0.5-million-year record of millennial-scale climate variability in the North Atlantic, *Science*, 283, 971–975, 1999.
- McManus, J. F., Francois, R., Gheradi, J.-M., Keigwin, L. D., and Brown-Leger, S.: Collapse and rapid resumption of Atlantic meridional circulation linked to deglacial climate changes, *Nature*, 428, 834–837, 2004.
- McNeil, B. I., Metzl, N., Key, R. M., and Matear, R. J.: An Empirical Estimate of the Southern Ocean air-sea CO₂ flux, *Eos Trans. AGU*, 87(36), Ocean Science Meeting Supplements, Abstract OS24G-02, 2006.
- Meissner, K. J., Schmittner, A., Weaver, A. J., and Adkins, J. F.: Ventilation of the North Atlantic Ocean during the Last Glacial Maximum: a comparison between simulated and observed radiocarbon ages, *Paleoceanography*, 18, 1023, doi:10.1029/2002PA000762, 2003.
- Monnin, E., Indermühle, A., Dällenbach, A., Flückiger, J., Stauffer, B., Stocker, T. F., Raynaud, D., and Barnola, J.-M.: Atmospheric CO₂ concentrations over the last glacial termination, *Science*, 291, 112–114, 2001.
- Morales-Maqueda, M. A. and Rahmstorf, S.: Did Antarctic sea-ice expansion cause glacial CO₂ decline?, *Geophys. Res. Lett.*, 29, 1011, doi:10.1029/2001GL013240, 2001.
- Munhoven, G.: Glacial-interglacial changes of continental weathering: estimates of the related CO₂ and HCO₃⁻ flux variations and their uncertainties, *Global and Planetary Change*, 33, 155–176, 2002.
- Paillard, D. and Parrenin, F.: The Antarctic ice sheet and the triggering of deglaciations, *Earth Planet. Sci. Lett.*, 227, 263–271, 2004.
- Petit, J. R., Jouzel, J., Raynaud, D., Barkov, N. I., Barnola, J.-M., Basile, I., Bender, M., Chappellaz, J., Davis, M., Delaygue, G., Delmotte, M., Kotlyakov, V. M., Legrand, M., Lipenkov, V. Y., Lorius, C., Pépin, L., Ritz, C., Saltzman, E., and Stievenard, M.: Climate and atmospheric history of the past 420,000 years from the Vostok ice core, *Antarctica, Nature*, 399, 429–436, 1999.
- Reimer, P. J., Baillie, M. G. L., Bard, E., Bayliss, A., Beck, J. W., Bertrand, C. J. H., Blackwell, P. G., Buck, C. E., Burr, G. S., Cutler, K. B., Damon, P. E., Edwards, R. L., Fairbanks, R. G., Friedrich, M., Guilderson, T. P., Hogg, A. G., Hughen, K. A., Kromer, B., McCormac, G., Manning, S., Ramsey, C. B., Reimer, R. W., Remmele, S., Southon, J. R., Stuiver, M., Talamo, S., Taylor, F. W., van der Plicht, J., and Weyhenmeyer, C. E.: INTCAL04 terrestrial radiocarbon age calibration, 0–26 Cal kyr BP, *Radiocarbon*, 46, 1029–1058, 2004.
- Ridgwell, A. J.: An end to the rain ratio reign?, *Geochemistry, Geophysics, Geosystems*, 4, 1051, doi:10.1029/2003GC000512, 2003a.
- Ridgwell, A. J.: Implications of the glacial CO₂ iron hypothesis for Quaternary climate change, *Geochemistry, Geophysics, Geosystems*, 4, 1076, doi:10.1029/2003GC000563, 2003b.
- Ridgwell, A. J. and Watson, A. J.: Feedback between aeolian dust, climate, and atmospheric CO₂ in glacial time, *Paleoceanography*, 17, 1059, doi:10.1029/2001PA000729, 2002.
- Riebesell, U., Zondervan, I., Rost, B., Tortell, P. D., Zeebe, R. E., and Morel, F. M. M.: Reduced calcification of marine plankton in response to increased atmospheric CO₂, *Nature*, 407, 364–367, 2000.
- Röthlisberger, R., Mulvaney, R., Wolff, E. W., Hutterli, M. A., Bigler, M., Sommer, S., and Jouzel, J.: Dust and sea salt variability in central East Antarctica (Dome C) over the last 45 kyrs and its implications for southern high-latitude climate, *Geophys. Res. Lett.*, 29, 1963, doi:10.1029/GL015186, 2002.
- Röthlisberger, R., Bigler, M., Wolff, E. W., Monnin, E., Joos, F., and Hutterli, M.: Ice core evidence for the extent of past atmospheric CO₂ change due to iron fertilization, *Geophys. Res. Lett.*, 31, L16207, doi:10.1029/2004GL020338, 2004.
- Sachs, J. P. and Anderson, R. F.: Increased productivity in the subantarctic ocean during Heinrich events, *Nature*, 434, 1118–1121, 2005.
- Sarnthein, M., Pflaumann, U., and Weinelt, M.: Past extent of sea ice in the northern North Atlantic inferred from foraminiferal paleotemperature estimates, *Paleoceanography*, 18, 1047, doi:10.1029/2002PA000771, 2003.
- Schmittner, A.: Decline of the marine ecosystem caused by a reduction in the Atlantic overturning circulation, *Nature*, 434, 628–633, 2005.
- Schwander, J., Jouzel, J., Hammer, C. U., Petit, J.-R., Udisti, R., and Wolff, E.: A tentative chronology for the EPICA Dome Concordia ice core, *Geophys. Res. Lett.*, 28, 4243–4246, 2001.
- Semiletov, I., Makshtas, A., and Akasofu, S.-I.: Atmospheric CO₂ balance: the role of Arctic sea ice, *Geophys. Res. Lett.*, 31, L05121, doi:10.1029/2003GL017996, 2004.
- Shackleton, N.: The 100,000-year ice-age cycle identified and found to lag temperature, carbon dioxide, and orbital eccentricity, *Science*, 289, 1897–1902, 2000.
- Shackleton, N. J., Berger, A., and Peltier, W. P.: An alternative astronomical calibration of the lower Pleistocene timescale based on OPD site 677, *Transactions of the Royal Society of Edinburgh: Earth Sciences*, 81, 251–261, 1990.
- Siddall, M., Rohling, E. J., Almogi-Labin, A., Hemleben, C., Meischner, D., Schmelzer, I., and Smeed, D. A.: Sea-level fluctuations during the last glacial cycle, *Nature*, 423, 853–858, 2003.
- Siegenthaler, U., Stocker, T. F., Monnin, E., Lüthi, D., Schwander, J., Stauffer, B., Raynaud, D., Barnola, J.-M., Fischer, H., Masson-Delmotte, V., and Jouzel, J.: Stable carbon cycle-climate relationship during the late Pleistocene, *Science*, 310, 1313–1317; doi:10.1126/science.1120130, 2005.

- Sigman, D. M. and Boyle, E. A.: Glacial/interglacial variations in atmospheric carbon dioxide, *Nature*, 407, 859–869, 2000.
- Smith, H. J., Fischer, H., Wahlen, M., Mastroianni, D., and Deck, B.: Dual modes of the carbon cycle since the Last Glacial Maximum, *Nature*, 400, 248–250, 1999.
- Stephens, B. B. and Keeling, R. F.: The influence of Antarctic sea ice on glacial-interglacial CO₂ variations, *Nature*, 404, 171–174, 2000.
- Stocker, T. F. and Johnsen, S. J.: A minimum thermodynamic model for the bipolar seesaw, *Paleoceanography*, 18, 1087, doi:10.1029/2003PA000920, 2003.
- Takahashi, T., Sutherland, S. C., Sweeney, C., Poisson, A., Metzl, N., Tilbrook, B., Bates, N., Wanninkhof, R., and Sabine, R. A. F., Olafsson, J., and Nojiri, Y.: Global sea-air CO₂ flux based on climatological surface ocean pCO₂, and seasonal biological and temperature effects, *Deep-Sea Res. II*, 49, 1601–1622, 2002.
- Toggweiler, J. R.: Variation of atmospheric CO₂ by ventilation of the ocean's deepest water, *Paleoceanography*, 14, 571–588, 1999.
- Toggweiler, J. R., I. Russell, J., and Carson, S. R.: Midlatitude westerlies, atmospheric CO₂, and climate change during the ice ages, *Paleoceanography*, 21, PA2005; doi:10.1029/2005PA001154, 2006.
- Vecsei, A. and Berger, W. H.: Increase of atmospheric CO₂ during deglaciation: constraints on the coral reef hypothesis from patterns of deposition, *Global Biogeochem. Cycles*, 18, GB 1035, doi:10.1029/2003GB002147, 2004.
- Vimeux, F., Cuffey, K. M., and Jouzel, J.: New insights into Southern Hemisphere temperature changes from Vostok ice cores using deuterium excess correction, *Earth Planet. Sci. Lett.*, 203, 829–843, 2002.
- Visser, K., Thunell, R., and Stott, L.: Magnitude and timing of temperature change in the Indo-Pacific warm pool during deglaciation, *Nature*, 421, 152–155, 2003.
- Watson, A. J. and Naveira-Garabato, A. C.: The role of Southern Ocean mixing and upwelling in glacial-interglacial atmospheric CO₂ change, *Tellus B*, 58B, 73–87, 2006.
- Wolff, E. W., Chappellaz, J. A., Fischer, H., Krull, C., Miller, H., Stocker, T., and Watson, A. J.: The EPICA challenge to the Earth System Modeling Community, *EOS*, 85, 363, 2004.
- Wolff, E. W., Kull, C., Chappellaz, J., Fischer, H., Miller, H., Stocker, T. F., Watson, A. J., Flower, B., Joos, F., Köhler, P., Matsumoto, K., Monnin, E., Mudelsee, M., Paillard, D., and Shackleton, N.: Modeling past atmospheric CO₂: results of a challenge, *EOS*, 86 (38), 341, 345, 2005.
- Wolff, E. W., Fischer, H., Fundel, F., Ruth, U., Twarloh, B., Littot, G. C., Mulvaney, R., Röthlisberger, R., de Angelis, M., Boutron, C. F., Hansson, M., Jonsell, U., Hutterli, M., Lambert, F., Kaufmann, P., Stauffer, B., Stocker, T. F., Steffensen, J. P., Bigler, M., Siggaard-Andersen, M. L., Udisti, R., Becagli, S., Castellano, E., Severi, M., Wagenbach, D., Barbante, C., Gabrielli, P., and Gaspari, V.: Southern Ocean sea-ice extent, productivity and iron fluxes over the past eight glacial cycles, *Nature*, 440, 491–496; doi:10.1038/nature04614, 2006.
- Wright, A. K. and Flower, B. P.: Surface and deep ocean circulation in the subpolar North Atlantic during the mid-Pleistocene revolution, *Paleoceanography*, 17, 1068, doi:10.1029/2002PA000782, 2002.
- Zeebe, R. E. and Westbroek, P.: A simple model for the CaCO₃ saturation state of the ocean: the Strangelove, the Neritan, and the Cretan Ocean, *Geochemistry, Geophysics, Geosystems*, 4, 1104, doi:10.1029/2003GC000538, 2003.
- Zeebe, R. E. and Wolf-Gladrow, D. A.: CO₂ in Seawater: Equilibrium, Kinetics, Isotopes, vol. 65 of Elsevier Oceanography Book Series, Elsevier Science Publishing, Amsterdam, The Netherlands, 2001.